

1 Research trends in the use of remote sensing for inland 2 water quality science: Moving towards multidisciplinary 3 applications

4 Simon Topp*¹, Tamlin Pavelsky¹, Daniel Jensen^{2,4}, Marc Simard², Matthew R.V. Ross³

5 ¹Department of Geological Sciences, University of North Carolina at Chapel Hill, 104 South Rd, Mitchell Hall,
6 Chapel Hill, NC 27599

7 ²NASA Jet Propulsion Laboratory, 4800 Oak Grove Dr, Pasadena, CA 91109

8 ³Department of Ecosystem Science and Sustainability, Colorado State University, 1476 Campus Delivery, Fort
9 Collins, CO 80523

10 ⁴Department of Geography, University of California at Los Angeles, Los Angeles, CA 90095, USA

11
12 * Corresponding Author – Simon Topp (Email: sntopp@live.unc.edu, Tel: 303-917-2694)

13 -Tamlin Pavelsky (pavelsky@email.unc.edu)

14 -Daniel Jensen (daniel.j.jensen@jpl.nasa.gov)

15 -Marc Simard (marc.simard@jpl.nasa.gov)

16 -Matthew Ross (mrvr@rams.colostate.edu)

17 **Abstract:** Remote sensing approaches to measuring inland water quality date back nearly 50 years to the
18 beginning of the satellite era. Over this time span, hundreds of peer reviewed publications have
19 demonstrated promising remote sensing models to estimate biological, chemical, and physical properties
20 of inland waterbodies. Until recently, most of these publications focused largely on algorithm
21 development as opposed to implementation of those algorithms to address specific science questions. This
22 slow evolution contrasts with terrestrial and oceanic remote sensing, where methods development in the
23 1970s led to publications focused on understanding spatially expansive, complex processes as early as the
24 mid-1980s. This review explores the progression of inland water quality remote sensing from
25 methodological development to scientific applications. We use bibliometric analysis to assess overall
26 patterns in the field and subsequently examine 236 key papers to identify trends in research focus and
27 scale. The results highlight an initial 30-year period where the majority of publications focused on model
28 development and validation followed by a spike in publications, beginning in the early-2000s, applying
29 remote sensing models to analyze spatiotemporal trends, drivers, and impacts of changing water quality
30 on ecosystems and human populations. Recent and emerging resources, including improved data
31 availability and enhanced processing platforms, are enabling researchers to address challenging science
32 questions and model spatiotemporally explicit patterns in water quality. Examination of the literature
33 shows that the past 10-15 years has brought about a focal shift within the field, where researchers are
34 using improved computing resources, data sets, and operational remote sensing algorithms to better
35 understand complex inland water systems. Future satellite missions promise to continue these
36 improvements by providing observational continuity with spatial/spectral resolutions ideal for inland
37 waters.

38 **Keywords:** remote sensing, water quality, lakes, rivers, inland waters, scientific advancement

1 1. Introduction

2 Remote sensing has long been promised as a tool for large-scale monitoring of inland water quality.
3 Dating back to the early 1970s, airborne and satellite sensors have been used to examine a wide range of
4 water quality constituents [1,2]. In the 50 years since, scientists have produced hundreds of peer reviewed
5 publications presenting models estimating biological, chemical, and physical properties of complex
6 waterbodies (see reviews [3–6]). Despite this proliferation of publications, existing reviews focus almost
7 exclusively on methodological approaches rather than on the scientific contributions of remote sensing to
8 our understanding of water quality, so characterization of the extent to which remote sensing has improved
9 our knowledge of inland water dynamics remains limited.

10 The historical tendency of inland water remote sensing to focus largely on methods development (here
11 defined as data collection and processing and/or algorithm calibration and validation), contrasts starkly
12 with that of related fields in terms of both the scope of research questions and the scale of studies. For
13 terrestrial remote sensing, algorithm development throughout the 1970s (e.g. Normalized Difference
14 Vegetation Index (NDVI) [7]) led to publications focused on spatially expansive, complex processes as early
15 as the mid-1980s. These papers include studies on global land use [8], global vegetation analysis [9], and
16 connections between primary productivity and carbon cycling [10,11]. For ocean color remote sensing,
17 early methods development led to global datasets and estimations of oceanic primary productivity by the
18 late 1980s [12,13]. Comparatively, global data products for inland water quality are limited, with a few
19 key exceptions (e.g. [14]) despite widespread acknowledgement of their importance from the inland water
20 scientific community [15,16]. This slow evolution can be partially explained by well-known challenges
21 related to remote sensing of complex waterbodies, as well as the limited availability of sensors appropriate
22 for inland water quality remote sensing [17], discussed in detail with other challenges in section 7.

23 Previous reviews have provided excellent summaries of the technical approaches available to retrieve
24 inland water quality parameters through remote sensing, as well as the current limitations of the field [3–
25 6,18–20]. Instead, we focus not on methodological details, but on the overall purpose and impact of past
26 publications, how those impacts have changed over time, and how the field may evolve in the future. We
27 quantify broad-scale trends through bibliometric analysis of search engine results. A subset of the most
28 relevant published papers (n=236) was identified using existing reviews, citation counts, database queries,
29 and journal-specific searches. The identified papers were subsequently read, with key attributes
30 documented in order to analyze trends and patterns in methodological approaches, model application,
31 research focus, and study scale over time. Here, trend refers to a pattern with directionality over time or
32 space. We limit our analysis to airborne and satellite remote sensing publications focusing on lakes, rivers,
33 deltas, and estuaries, although we fully acknowledge that these publications were preceded by years of
34 vital methods development using handheld and shipborne sensors (e.g. [21–26]). Similarly, given the
35 focus of this paper on the remote sensing of lake, river, delta, and estuarine systems, which present their
36 own unique challenges [17], we excluded studies on near shore ocean waters and the Laurentian Great
37 Lakes.

38 Our results highlight a nearly 30-year period focusing predominantly on methods development prior
39 to a spike in publications, beginning in the early 2000s, applying well validated algorithms to identify
40 spatiotemporal trends, drivers, and impacts of changing inland water quality on ecosystem functions and
41 human populations. Study scale exhibits a similar trend towards increasingly large areas with more
42 waterbodies studied over longer periods of time, slowly moving closer to regional and global-scale data
43 products. Through both broad and detailed inspection of the field, our results suggest that the past decade
44 of inland water remote sensing has led to a fuller understanding of inland water processes by focusing on

45 challenging science questions and increased study scales. This contribution continues today with an ever-
46 expanding body of available data, processing platforms, and methodologies.

47 We contextualize our analysis of the literature by: 1) summarizing the primary water constituents
48 measured with earth observation instruments, 2) providing a brief overview of common modelling
49 approaches to measure those constituents, and 3) discussing the limitations that have hampered past
50 research. This contextual information is followed by the bibliometric and index analysis described above.
51 We conclude with a discussion of potential future directions for the field.

52 **2. Earth observation sensors and optically active waterbody constituents**

53 The work reviewed here focuses primarily on passive optical satellite sensors capable of large-scale
54 remote sensing research. In general, these are either ocean color sensors such as the Moderate Resolution
55 Imaging Spectroradiometer (MODIS) [29–32], the Medium Resolution Imaging Spectrometer (MERIS) [33–
56 36], and the Sentinel-3 Ocean and Land Cover Instrument (OLCI) [37], or land surface optical sensors
57 including the Landsat series (Multispectral Scanner (MSS): [38–40]; Thematic Mapper (TM): [41–43];
58 Enhanced Thematic Mapper (ETM+): [44–46]; and Operational Land Imager (OLI): [47,48]), Sentinel 2 A/B
59 MultiSpectral Instrument (MSI) [49,50], and SPOT High Resolution Geometric Sensor (HRG) [51]. A
60 subset of researchers have used high resolution commercial sensors including WorldView 2 [52] and
61 IKONOS [53,54]. The above sensors vary significantly in their applicability based largely on their spatial,
62 temporal, spectral, and radiometric resolutions. Temporal and spatial resolutions determine the scale of
63 processes that can be captured by a given sensor. In general, land surface sensors have a finer spatial
64 resolution (~10m - 30m) but coarser temporal resolution (~1-2 weeks), allowing them to detect spatial
65 patterns in water quality in smaller waterbodies (e.g. small lakes and rivers) but with only 1-2 observations
66 per month depending on the sensor and cloud cover conditions. Comparatively, ocean color sensors are
67 characterized by coarse spatial resolutions (~300-1000 m) but finer temporal resolutions (~daily), limiting
68 observations to large waterbodies but facilitating examination of processes that occur at short timespans.
69 A more in-depth discussion on the effects of varying resolutions across ocean and terrestrial sensors can be
70 found in Olmanson, Brezonik, & Bauer (2011)[55] and CEOS (2018)[56].

71 Since water is highly absorptive within the near and shortwave infrared spectrum, the majority of
72 water-leaving radiance occurs within the visible spectrum with slight variations dependent on temperature
73 and salinity [57,58]. The primary exception is in optically complex waters (due to high turbidity and/or
74 bottom reflectance), where sediment reflectance exceeds the absorptive properties of water in the near and
75 shortwave infrared wavelengths [51,59]. Relatively high absorption within the visible spectrum leads to
76 a low range of reflectance values when compared to land surface remote sensing. This low range requires
77 high sensitivity (i.e. high radiometric resolution) to detect small changes in reflectance [4]. Different
78 concentrations of varying water quality parameters lead to various absorption and backscattering peaks
79 within the water leaving radiance. The spectral resolution, measured by the range of wavelengths
80 captured by individual sensor bands, needs to be sufficiently fine to capture spectral peaks and accurately
81 estimate the contribution of a given water quality parameter to the overall spectral signature [17]. The
82 sensors mentioned above are all multispectral sensors, meaning that they have a small number of relatively
83 wide bands (~10 nm to ~80 nm) placed within the visible to mid-infrared spectrum. These coarse
84 bandwidths can complicate retrieval of water quality parameters [17]. In order to better capture the
85 specific absorption and backscattering peaks within a waterbody's spectral signature, a subset of
86 publications have utilized hyperspectral sensors that provide hundreds of narrow (1- 10 nm), contiguous
87 bands spanning the visible to shortwave infrared spectrum (see [60]). Currently, the majority of
88 hyperspectral sensors are airborne or in planning stages for future satellite missions [61]. Within inland
89 water remote sensing, applications of hyperspectral remote sensors include the use of Hyperion [62,63], the

90 Compact Airborne Spectrographic Imager (CASI) [64,65], the Airborne Prism Experiment (APEX) [66], and
91 NASA's HyMAP scanner [67], Airborne Visible/Infrared Spectrometer (AVIRIS) [68], Airborne
92 Visible/Infrared Spectrometer-Next Generation (AVIRIS-NG) [69], and Portable Remote Imaging
93 Spectrometer (PRISM) [70].

94 Regardless of sensor, the optically active water parameters that contribute to the total water-leaving
95 signal are phytoplankton, organic and inorganic suspended sediments, and colored dissolved organic
96 matter (CDOM). [59,71,72]. The sum of these three individual constituents, in combination, attribute to
97 differences in overall water clarity, which is frequently used as a proxy for water quality [15,73].
98 Publications leveraging relationships between optically inactive constituents, which have no detectable
99 spectral signal, and the optically active constituents listed above have provided remote sensing models for
100 nitrogen and phosphorous [74–76], dissolved oxygen [41,49], and heavy metals [77]. However, compared
101 to optically active parameters, these optically inactive constituents require site specific algorithms due to
102 varying regional correlations with optically active water quality constituents. Publications examining the
103 remote sensing of inactive constituents date back to the early 90s [42,78]; however, they appear relatively
104 infrequently within the literature and are not discussed in detail here. Below, we describe the optically
105 active constituents with their distinct spectral signatures.

106 2.1 *Chlorophyll-a*

107 Chlorophylls are the photosynthetically active compounds that convert light into energy for
108 photosynthesis. Remote sensing studies primarily focus on chlorophyll-a (chl-a), which is the most
109 abundant chlorophyll and is present within all plants, algae, and cyanobacteria that photosynthesize. In
110 aquatic systems, it is used as a proxy measure of total algal biomass [79]. The algal biomass of a waterbody
111 controls its overall biological productivity, also known as trophic state, making it an ideal indicator of
112 ecosystem integrity [80,81]. While not all algal blooms are inherently harmful, blooms containing certain
113 species, most commonly phycocyanin-producing cyanobacteria, are toxic to humans, livestock, and
114 wildlife [82]. Anthropogenically driven nutrient loading and climate change in recent decades have
115 increased the size and frequency of these harmful algal blooms worldwide [83].

116 Optically, the spectral signature of chl-a varies depending on its concentration in relation to other
117 water quality parameters and the composition of phytoplankton phenotypes producing the signal [84,85].
118 For low biomass, oligotrophic to mesotrophic waterbodies, the chl-a spectrum is characterized by a sun-
119 induced fluorescence peak around 680 nm [86–88]. For high biomass, eutrophic waterbodies, the
120 florescence signal is masked by absorption and backscattering peaks centered at 665 nm and 710 nm
121 respectively [89]. The ratio between these two wavelengths has been used to accurately estimate chl-a
122 concentrations in numerous studies [90–92]. Beyond basic constituent retrieval, research focusing on
123 chlorophyll includes the detection of harmful cyanobacteria [93–95] and phycocyanin [64,96], assessment
124 of trophic state [46,47,97], and algal bloom development and dispersion modelling [98–101].

125 2.2 *Total Suspended Solids*

126 Total suspended solids refer to both inorganic and organic particles held in suspension throughout a
127 water column. Controls on the composition of organic and inorganic particles vary geographically, with
128 some areas driven primarily by inorganic sediments and others by phytoplankton. In the literature it is
129 referred to variously as total suspended matter, suspended sediment concentration, and particulate matter,
130 though the precise definitions of these terms sometimes vary. Monitoring TSS fluxes has strong
131 implications for biogeochemical cycling in terms of nutrient transport [102], heavy metal loading [103],
132 light conditions [104], and global carbon budgets [105]. Terrestrial carbon deposition into lakes and
133 reservoirs, largely in the form of TSS, is double that of deposition into the ocean [106,107], despite lakes

134 comprising only 3% - 3.7% of the total land area [108,109]. Simultaneously, the settling out of TSS into
135 lake bottom sediments provides a carbon sink, with current global carbon sequestration estimates ranging
136 from 0.06-0.27 Pg year⁻¹ [105,107]. On a local scale, high TSS reduces light penetration through increasing
137 turbidity and leads to benthic smothering, impacting species composition and primary productivity from
138 macrophytes [110,111]. Finally, TSS concentrations and flux in rivers capture the landscape processes
139 controlling delivery of erosional products from land to ocean [112,113].

140 Spectral signatures of TSS concentrations can vary significantly based on the particle size and
141 composition of organic to inorganic materials [114,115]. Organic-dominated systems derive their spectral
142 signatures from algae concentrations and can share the pronounced absorption and backscattering peaks
143 described above for chlorophyll [116]. As inorganic TSS concentrations increase within a waterbody, the
144 location of the spectral maximum moves from around 550 nm into the red or near-infrared wavelengths
145 [51] with waterbody specific variation dependent on chlorophyll and CDOM concentrations. Remote
146 sensing studies examining TSS focus largely on riverine and coastal systems, with notable studies including
147 estimates of TSS delivery to the ocean [112], variability in sediment plume size [28,30,117], impacts of
148 reservoirs on sediment concentration [118], impacts of land use change on sediment delivery [119], and
149 variability of sediment in lagoons [120]. TSS concentrations can be correlated with various optically
150 inactive water quality parameters and have subsequently been used to infer the concentration of
151 phosphorous [3], mercury [119], and other metals [67] at local scales.

152 2.3 Colored Dissolved Organic Matter

153 Colored (or ‘chromophoric’) dissolved organic matter is the colored portion of total dissolved organic
154 carbon. Sources of CDOM can be either autochthonous (i.e. phytoplankton) or allochthonous (i.e.
155 terrestrial carbon). Of the two sources, allochthonous carbon leached out of surrounding soils is generally
156 the dominant control of total lake and river dissolved organic carbon [121]. Photo and biodegradation of
157 CDOM can contribute to elevated levels of CO₂ within lacustrine systems [122]. Recent studies of CO₂
158 concentrations in Chinese [123] and US [124] lakes found that ~60-70% were supersaturated with CO₂.
159 Globally, this oversaturation leads to 0.35 – 0.43 Pg year⁻¹ of carbon off-gassed into the atmosphere, in
160 addition to an estimated 1.8 Pg year⁻¹ emitted from streams and rivers [125]. At low levels, CDOM absorbs
161 harmful ultraviolet radiation with minimal impact on light penetration within the visible spectrum [126].
162 As concentrations increase, absorption of low-wavelength light by CDOM regulates the light availability
163 of primary producers, controlling net productivity and trophic structure [126,127]. Continued monitoring
164 of CDOM directly, and as a proxy for total dissolved organic carbon, provides a better understanding of
165 carbon inputs and processing in freshwater systems.

166 Highly absorptive in the visible spectrum, elevated levels of CDOM lead to stratified, dark
167 waterbodies with limited light penetration [128]. Similar to TSS, the reflectance spectra of waterbodies
168 with varying concentrations of CDOM are highly dependent on the composition of other optically active
169 constituents, and in certain areas can be complicated by the presence of colloidal iron, which shares similar
170 optical properties [129]. CDOM’s contribution to water-leaving radiance is characterized by an
171 exponential increase in absorption as wavelength decreases [130]. Intuitively, this would suggest that
172 CDOM models should incorporate wavelengths in the blue spectrum; however, excessive absorption by
173 CDOM and low natural water-leaving radiance at low wavelengths reduces the usable signal [24,131]. As
174 a result, algorithms commonly incorporate a green/red ratio (e.g. [49,132–134]). Remote sensing studies
175 focusing on CDOM range in application from identifying trends in inland water carbon content [135,136]
176 to examining landscape-level drivers of CDOM distributions [52,137]. Work in rivers highlights controls
177 of carbon export in arctic landscapes [138] and relationships governing CDOM variation in river estuaries

178 along with the resulting impact on correlated concentrations of methylmercury [70]. An in depth review
179 of CDOM and its optical properties was published by Coble (2007) [139].

180 2.4 Water Clarity

181 The combination of chlorophyll, suspended sediments, and CDOM collectively contribute to overall
182 water clarity. Most commonly, Secchi Disk depth or turbidity are used as relative measures of clarity.
183 The former metric, developed more than 150 years ago, quantifies the maximum visible depth of a white
184 and black disk lowered into a waterbody [140,141]. In comparison, turbidity is an explicit measurement
185 of light scattering within a water column caused by suspended and dissolved particles. Water clarity
186 regulates freshwater ecosystems through light attenuation and control over epilimnion depth [142].
187 Numerous studies have examined the role of water clarity in thermal stratification [143,144], lake
188 metabolism [145,146], and biodiversity [110]. Generally, a shallower thermocline and reduced light
189 penetration associated with degraded water clarity reduces photosynthesis of submerged macrophytes and
190 other primary producers [110,147].

191 Remote sensing retrievals of water clarity almost universally use wavelengths and band ratios that
192 include the red spectrum in some way (e.g. [73,78,148–153]). Reflectance at these wavelengths accounts
193 for total sediment and chlorophyll concentrations such that increasing brightness is associated with
194 decreased water clarity [4]. Water clarity has long been acknowledged as a proxy for nutrient availability
195 and chlorophyll concentrations within lakes [154–156]; as a result, remote sensing studies frequently use it
196 as a proxy for overall lake trophic status (oligotrophic, mesotrophic, or eutrophic) [97,157,158].

197 3. Modelling approaches

198 Models that leverage the relationship between a waterbody's optical qualities and its concentration of
199 optically active water quality constituents are commonly referred to as bio-optical algorithms [153]. In
200 inland waters, these models can be categorized as empirical, semi-analytical, or machine learning based.
201 While inherently empirical, we distinguish machine learning techniques separately due to their
202 computational complexity and ability to handle non-linear relationships. As discussed below, all three of
203 these modeling approaches have benefits and shortcomings in terms of applicable scale, model
204 transparency, and model complexity.

205 3.1 Empirical models

206 The most common approach to inland water remote sensing involves fitting a standard linear
207 regression between spectral band/band ratio values and temporally coincident *in situ* water quality
208 measurements. One inherent limitation of this approach is its non-generalizability across large spatial and
209 temporal scales where variations in atmospheric and water composition create large variability in observed
210 spectral signatures of water quality parameters. As such, empirical models are restricted to confident
211 predictions only within the range and setting of the input data. This restriction limits their application
212 across spatiotemporal domains. At a local scale, empirical modelling accounts for the site-specific optical
213 qualities of the water, but with increasing spatial or temporal scales, optically non-homogenous
214 waterbodies and changing atmospheric conditions complicate parameterization [159]. These
215 shortcomings are often outweighed by the benefits of model transparency, simplicity, and minimal
216 computational requirements.

217 The family of empirical models can be split into purely empirical and semi-empirical approaches.
218 The purely empirical approach derives relationships using input band and band ratio values as coefficients,
219 often generating multiple models and choosing the best fit through comparison of error metrics. Purely

220 empirical approaches date back to the 1970s and 80s, with notable applications examining trophic state in
 221 Wisconsin [2] and Minnesota [75], and turbidity and chlorophyll in Australian lakes [160].

222 In contrast, semi-empirical models use multi-band index values with some basis in the physical
 223 properties of the constituent of interest. These models largely focus on the measurement of water clarity,
 224 chl-a, cyanobacteria, and TSS. Like terrestrial vegetation indices (e.g. NDVI), they are designed to enhance
 225 the spectral properties of the constituent of interest while reducing noise from extraneous optical
 226 parameters; however, unlike semi-analytical approaches (described below), semi-empirical models don't
 227 incorporate any inverse modelling of the inherent optical properties of a given waterbody. Notable semi-
 228 empirical indexes include the normalized difference chlorophyll index [161], the maximum chlorophyll
 229 index [162], the Floating Algal Index [163], and the normalized difference suspended sediment index [164].
 230 Application of these semi-empirical indexes has contributed to robust algal bloom detection [165],
 231 determining the presence of harmful cyanobacteria concentrations associated with eutrophication [84], and
 232 modelling sediment concentrations in rivers and deltas [164]. Due to their basis in physical properties,
 233 semi-empirical models are more generalizable than purely empirical approaches. However, they
 234 necessitate measurements of specific wavelengths that capture absorption and scattering peaks, restricting
 235 their applicability to sensors with suitably placed band centers and sufficient spectral resolution.

236 3.2 Semi-analytical models

237 Analytical and semi-analytical models are physics based and involve parameterization based on the
 238 inherent optical properties (IOPs) of water and the atmosphere, where IOPs refer to the optical properties
 239 of the medium of interest that are independent of the ambient light field [59,71]. The IOPs of a given
 240 waterbody are modelled in coordination with apparent optical properties (including illumination
 241 conditions, sensor orientation, and field of view) to construct theoretical absorption and backscattering
 242 values which can then be decomposed through an inverse equation to estimate optically active water
 243 quality constituents (described below)[18,59,72,166]. For purely analytical models, the inverse equation is
 244 parameterized based purely on light physics; however, these are rarely used for optically complex waters
 245 where the interactions of numerous water quality constituents become difficult to model. As a result,
 246 semi-analytical models, which incorporate *in situ* measurements to parameterize the inverse equation, are
 247 the primary form of physics based algorithms developed for inland water quality remote sensing retrievals
 248 [4]. This modelling approach evolved from the reflectance approximation developed by Morel and Prieur
 249 (1977)[167], who studied turbidity and chlorophyll in ocean waters. Compared to empirical and semi-
 250 empirical algorithms, semi-analytical models are mechanistic, make a priori assumptions regarding light
 251 physics, and are theoretically generalizable outside the range of a given study; however, the application of
 252 any single model to optically nonhomogeneous waterbodies requires large amounts of *in situ* validation
 253 data and remains challenging [16].

254 A prerequisite to this modelling approach is understanding the light physics that control reflectance
 255 as particle size, composition, and concentration vary. These properties are modelled through the
 256 absorption and backscattering coefficients of all the optically active constituents found within the study
 257 area (Eq. 1). While derivations of semi-analytical models come from numerous sources (e.g. [27,168–
 258 170]), the basic form of the preliminary equation follows equation 1.

$$259 \text{ Eq. 1 } R(\lambda) = Y * \frac{b(\lambda)}{a(\lambda) + b(\lambda)}$$

260 Here, the total reflectance just below the water's surface (R) at wavelength λ is equal to the
 261 backscattering at the given wavelength over the absorption plus the backscattering at the given wavelength
 262 times an empirically or analytically derived constant Y . The absorption and backscattering coefficients
 263 can be further broken down into absorption and backscattering for each optically active constituent. (e.g.

264 $b(\lambda) = b_{water}(\lambda) + b_{cdom}(\lambda) + (\lambda)b_{chl} + (\lambda)b_{tss}$. Values for R are either generated through *in situ*
265 measurements of reflectance and water quality or theoretically generated using physical modelling
266 software such as HydroLight [171]. These generated spectral signatures are then used to parameterize an
267 inverse model that decomposes R into optically active constituent concentrations through their absorption
268 and backscattering coefficients. One benefit of this inverse modelling procedure is the ability to estimate
269 multiple water quality parameters simultaneously. However, model development is inherently
270 complicated and, depending on if atmospheric corrections have been applied, requires information about
271 atmospheric composition, bottom reflectance, and extensive *in situ* sampling. Even so, the literature
272 contains numerous examples of successful applications of semi-analytical models across large
273 spatiotemporal scales. Early development of semi-analytical modelling for inland waters was led by
274 researchers such as Dekker [26,172] and Kutser [173] examining chl-a, TSS, and CDOM. More recently,
275 Heege et al. (2014)[174] developed a semi-analytical algorithm for turbidity across the Mekong Delta with
276 strong validation results using MODIS, Landsat, and RapidEye, Lymburner et al. (2016)[175] applied a
277 semi-analytical algorithm to a multi-decadal study of TSS in Australian lakes, and both Volpe et al.
278 (2011)[120] and Zhou et al. (2017)[176] applied semi-analytical algorithms across multi- and hyper-spectral
279 data to detect TSS in shallow lagoons. For a more detailed description of semi-analytical modelling see
280 Dekker, Vos, & Peters (2002)[178], Giardino et al. (2019)[18], Morel (2001)[166], and IOCCG (2000)[59].

281 3.3 Machine learning models

282 In recent years, increases in computational capacity and available data have created opportunities for
283 novel approaches to data analysis. While inherently empirical, machine learning approaches are
284 differentiated by their ability to operate in multidimensional space with complex non-linear relationships
285 [179]. The spectrum of machine learning methods for remote sensing applications is broad [180,181]; here,
286 we focus on the benefits and limitations of machine learning methods generally, along with some notable
287 examples in the field of inland water remote sensing. A more detailed review of machine learning
288 methodology for remote sensing was published by Lary et al. (2016)[181].

289 Within inland water remote sensing, machine learning algorithms including artificial neural networks
290 [182–184], genetic algorithms/programming [185,186], support vector machines [187], random
291 forest/boosted regression trees [188], and empirical orthogonal functions [189,190] have all shown promise
292 in accurately estimating water quality parameters across a variety of spatiotemporal scales. As with
293 traditional empirical models, machine learning approaches are only applicable within the range and setting
294 of data used to train a given model. However, unlike traditional empirical models, most machine learning
295 models use iterative learning to reduce overall error and maximize model fit [191]. Depending on the
296 parameterization of the model and the amount of training data available, this approach may lead to over-
297 fitting of the data, especially in models with numerous input variables subject to collinearity such as
298 adjacent hyperspectral bands [192]. To avoid overfitting, machine learning methods require the provision
299 of separate training and testing datasets that contain representative samples of the parameters of interest.
300 The power and scalability of most machine learning algorithms is dependent on the quality and range of
301 the training and testing data. Given the proper inputs, these algorithms can produce generalizable models
302 that capture complex, non-linear relationships between remotely sensed reflectance and biogeophysical
303 parameters. While modelling chl-a and turbidity in Lake Chagan, China, Song (2011)[183] found
304 reductions in root mean square error of 76% and 65%, respectively, when comparing traditional regression
305 techniques to artificial neural networks. Similarly, Xiang et al. (2015)[193] found a 20% increase in trophic
306 state classification accuracy when using machine learning compared to multivariate regression.

307 4. Challenges and limitations within the field

308 Despite the diverse modelling approaches discussed above, several barriers still exist that limit the
309 progress of inland water remote sensing. Sensor design, atmospheric effects, dynamic waterbodies, and
310 institutional barriers all present legitimate challenges to increasing the scale and robustness of remote
311 sensing algorithms.

312 At the most basic level, many sensors are limited in the types of observations they can make.
313 Multispectral, broad-band satellites like the Landsat TM/ETM+ series were engineered for terrestrial
314 applications and lack the spectral resolution and band centers ideal for complex waters. Their relatively
315 infrequent return periods make them more suited to detecting long-term changes as opposed to daily or
316 weekly variation. Ocean color sensors including MODIS, SeaWiFS, and MERIS have higher spectral
317 resolution and frequent return periods, but they lack the spatial resolution to capture narrower inland
318 water bodies, particularly rivers (see [4,17] for detailed discussion). The newest generation of sensors has
319 been designed to overcome some of these issues [18,19], though the limited precision of broad spectral
320 bands remains a challenge. While they lack certain band centers useful for inland water remote sensing,
321 new sensors such as the Landsat 8 Operational Land Imager (OLI) and the Sentinel 2 MultiSpectral
322 Instrument (MSI) have increased signal to noise ratios, improved radiometric and temporal resolution, and
323 aerosol-specific bands making them better equipped to handle the size and complexity of inland waters
324 [194,195].

325 Regardless of sensor choice, among the largest barriers to remote sensing of inland waters is
326 controlling for varying atmospheric effects. The signal to noise ratio of top-of-atmosphere radiance over
327 waterbodies can vary substantially with different atmospheric water vapor and aerosol concentrations. In
328 order to accurately estimate water quality parameters, the atmospheric effects need to be controlled for
329 through precise atmospheric corrections [20,196]. These corrections are particularly important over large
330 spatiotemporal domains because atmospheric conditions can vary significantly. Historic correction
331 procedures are largely based on open ocean remote sensing and assume zero water leaving radiance
332 beyond the visible spectrum [197]. This assumption does not hold over optically complex waters where
333 chlorophyll, suspended sediment, and bottom reflectance lead to true non-zero radiance in the near
334 infrared. The result is an overestimation of aerosol thickness and an overcorrection of visible wavelengths
335 in turbid waters [198]. Progress has been made improving atmospheric correction algorithms over
336 complex waters through the use of radiative transfer functions [198], pseudo-invariant features [194], dark
337 pixel extraction [199], and SWIR-based correction procedures [200,201]; however, many methods lack
338 transferability between sensors making it difficult to compare surface reflectance products across platforms
339 [202]. Atmospheric correction is further complicated by adjacency effects from surrounding land.
340 Radiation reflected from relatively bright land is scattered by the atmosphere, increasing noise over
341 adjacent, relatively dark waterbodies. Solving adjacency issues typically involves computationally
342 expensive radiative transfer functions, though recent progress has been made using models that reduce
343 computational requirements by approximating atmospheric scattering within the correction procedure
344 [203].

345 Independent atmospheric challenges are exacerbated by the dynamic nature of waterbodies
346 themselves. Changing water conditions and bio-fouling of *in situ* sensors can make it difficult to capture
347 coincident field and satellite observations necessary for model development [204,205]. From a reflectance
348 standpoint, algal mats, surface macrophytes, and sun glint (specular reflection of sunlight towards the
349 sensor) all contribute extraneous signals to observed water-leaving radiance. The body of literature on
350 these issues is significant, and processing schemes to isolate and/or remove these signals are continually
351 improving. For sun glint, removal schemes can range from relatively simple empirical models such as
352 those tested by Kutser, Vahtmäe, & Praks (2009)[206] to more complicated radiative transfer functions [207].
353 For algal mats and floating macrophytes, semi-empirical threshold-based algorithms including the Floating

354 Algal Index [163], Maximum-Peak Height [89], and adaptations of classic NDWI indexes [94] have all
355 provided robust delineation of water from adjacent algal and macrophyte signals. Additionally, varying
356 sediment types between regions can affect the relationship between reflectance and measurements of TSS
357 [115]. These variations can be partially accounted for using band ratio algorithms that are generalizable
358 across sediment types [208].

359 The above technical barriers represent legitimate challenges to extracting water quality constituents
360 from dynamic inland systems. However, existing retrospectives on the past 50 years in the field indicate
361 that technical barriers alone are not responsible for the slow progress towards applying remote sensing as
362 a tool to better understand inland water systems. Bukata (2013)[209] insightfully proposes that one
363 explanation may be the relatively isolated nature of the field and the historic lack of collaboration with
364 related ocean color remote sensing. This observation is supported by Downing (2014)[210], who describes
365 the fields of oceanography and limnology as “twins, mostly separated since birth”. This lack of
366 institutional communication has had ripple effects, reducing collaborative projects and limiting funding
367 sources. Collaboration is further reduced through the inherent scale of the research. Technical
368 challenges with spatiotemporally expansive studies generally constrain inland water research efforts to
369 localized scales. This pattern contrasts with ocean remote sensing, where international study areas have
370 led to numerous, well-funded, multinational research efforts [211]. Communication and collaboration
371 leading to these large research efforts is facilitated by international organizations like the International
372 Ocean-Colour Coordinating Group (IOCCG). Recent work done by the IOCCG [20], as well as emerging
373 groups like AquaWatch (<https://www.geoaquawatch.org/>), are working towards similar goals for inland
374 water remote sensing researchers, but these efforts are still in their infancy compared to their ocean color
375 counterparts. The nature of the field and its apparent lack of cohesion may, in part, stem from the fact
376 that it is spread across many different disciplines. A Scopus search query of inland water quality remote
377 sensing returns publications from over 350 distinct journals spread across hydrology, ecology,
378 biogeochemistry, environmental management, and engineering, indicating that much of the research is
379 spread across different niches and sub-disciplines. However, the following examination of the literature
380 indicates that these barriers, both technical and institutional, have been dramatically reduced over the past
381 decade.

382 5. Evolution of inland water remote sensing publications

383 In order to analyze the progression of publications on remote sensing of inland water quality, we
384 carried out two analyses: the first identifies general trends in publication patterns, while the second
385 analyzes trends in modelling approaches and research focus.

386 5.1 Overarching trends in the field of
387 inland water remote sensing

388 General trends were identified
389 through a bibliometric analysis of
390 search results from the Elsevier
391 Scopus database (conducted July
392 2018). Database titles, keywords,
393 and abstracts were searched for the
394 terms 'remote sensing', 'water
395 quality', and either 'lake', 'reservoir',
396 'river', 'delta', 'estuary', or 'inland
397 waters' (along with variants, i.e. 'lake'
398 and 'lakes'). The search results
399 returned 1,186 distinct articles
400 published in peer reviewed journals
401 dating back to 1970 (Figure 1).
402 Bibliometric data was extracted from
403 the query using the Bibliometrix
404 package in R [212].

405 The results of the Scopus
406 bibliometric analysis indicate that
407 inland water quality remote sensing
408 has been growing dramatically since
409 its introduction in the 1970s. The
410 annual average increase in publications
411 over the study period is 8.9%, but
412 examination of the trend indicates
413 that it is best represented by a
414 simple power law function ($R^2 = 0.848$),
415 with a sharp increase in
416 publications starting in the early
417 2000s. Power law functions allow
418 for the calculation of a doubling
419 time which represents the amount
420 of time it takes a population to
421 double in size starting from any
422 given timepoint. Bornmann & Mutz
423 (2015) calculated the doubling time
424 and average annual growth rate for
425 total academic publishing between
426 1980 and 2012 to be approximately
427 23.7 years and 2.96% respectively.
428 For the same period, remote sensing
429 of inland water quality grew at
430 three times that rate, with a
431 doubling time and average annual
432 growth rate of 8.3 years and 10.01%
433 respectively. The most pronounced
434 year-on-year jump occurs right
435 after 2008, which corresponds to
436 the public release of freely available
437 Landsat imagery by NASA and the
438 US Geological Survey. After
439 removing the overall trend of the
440 power law function, a t-test on the
441 residuals for the 5 years before and
442 after 2008 indicates a significant
443 increase in publications for the
444 period after Landsat was made
445 public (95% CI = 0.3-0.7, $p = 0.0016$).
446 This result is consistent with
447 previous research showing that for
448 multiple earth observation fields,
449 the release of the Landsat archive
450 resulted in more frequent and
451 larger-scale studies [214].

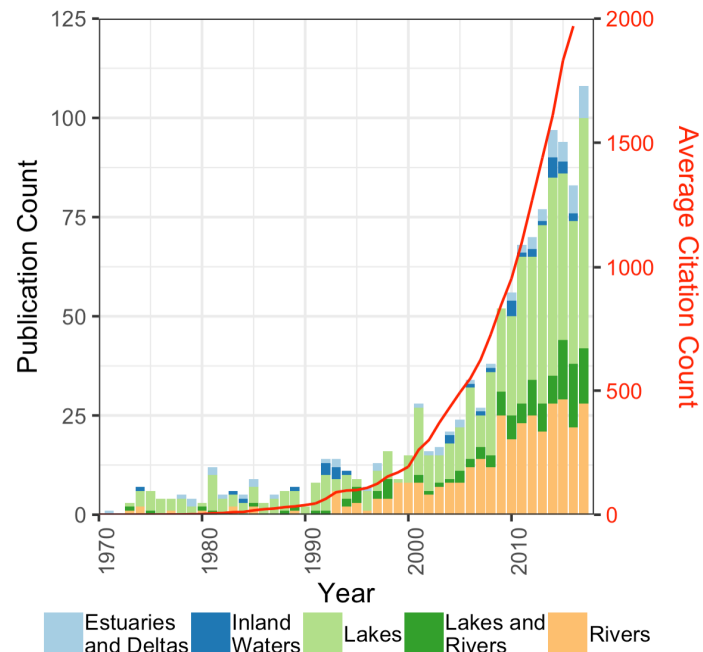


Figure 1. Published papers per year returned from Scopus search queries and grouped by search term. Average citation count is the sum of citations for all papers averaged over the number of years since their publication.

424 Further analysis of the bibliometric data shows that while contributions to the literature come from a
 425 diverse set of sources, there are a few distinct countries, journals, and authors that are disproportionately
 426 active within the field. Publications from the United States and China are responsible for 26.1% and 21.4%
 427 of the total publications respectively (Figure 2). Similarly, while there are contributions to the literature
 428 from 3,362 authors or co-authors, publications that include the top ten most productive authors comprise
 429 17% of the total search results (Table 1). The cumulative contribution of publications from the top ten

Table 1. Summary data from Scopus query for inland water quality remote sensing.

Scopus Query Summary	
Total Publications	1186
Distinct Journals	342
Distinct Key words (Scopus)	7706
Distinct Key words (Authors)	2447
Average citations per publication	16.6
Authorship Summary	
Distinct Authors	3,362
Authors per Documents	5.24
Contributions Summary	
Contribution from top 10 Countries	676 (54.8%)
Contribution from top 10 Authors	209 (16.9%)
Contribution from top 10 Journals	378 (30.6%)

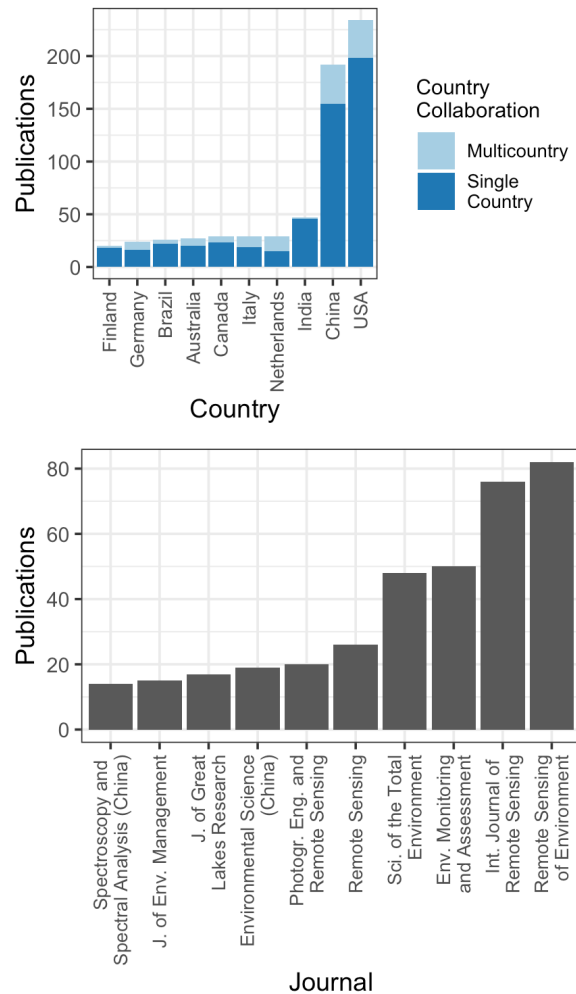


Figure 2. Distribution of publications returned from Scopus query for the top ten most productive countries and top ten most published journals.

430 journals comprise nearly one third of the entire
 431 search. Of the 378 publications from these top ten
 432 journals, 60% are from strictly remote sensing
 433 journals. When expanded out to the entire query,
 434 18% of the returned journals include a remote
 435 sensing term in their title and account for 33% of
 436 all publications. This pattern is worth noting for
 437 two reasons. First, remote sensing journals are
 438 more likely to contain methods development
 439 papers. Secondly, it suggests that many
 440 publications are focused primarily on
 441 communicating advances within the remote
 442 sensing community, with perhaps less outreach to
 443 hydrologists, ecologists, and other scientists not
 444 inherently focused on remote sensing.

445 5.2 Detailed analysis of literature patterns and scale

446 In order to more deeply examine trends in remote sensing of water quality, we identified a subset of
 447 236 papers within existing reviews [3–5] and from keyword searches containing common inland water
 448 remote sensing terms (e.g. combinations of 'remote sensing', 'lakes', 'rivers', 'chlorophyll', 'CDOM', 'TSS',
 449 and 'inland waters') in relevant databases (Article+, Google Scholar, Scopus, and Web of Science). Papers

450 were chosen based on a combination of their search relevance, citation count, and subject focus. While we
 451 strived to be comprehensive in the inclusion of papers, some relevant studies were inevitably missed. We
 452 conducted more intensive journal-specific searches within high impact journals including Science, Nature,
 453 PNAS, WRR, Association for the Sciences of Limnology and Oceanography (ASLO) journals, and
 454 Ecological Society of America (ESA) journals to ensure the inclusion of studies that utilized remote sensing
 455 but focused more on scientific application of remote sensing than on methods development. A significant
 456 and worthwhile body of work exists using remote sensing to study water quality in complex near coast
 457 ocean environments as well as the Laurentian Great Lakes (see reviews [3–6]). While critical to the
 458 development of inland water quality remote sensing methods, this body of work was excluded from this
 459 review in order to better focus on lake, river, and estuary remote sensing applications and how those
 460 applications have changed over time. Similarly, studies using strictly *in situ* reflectance were excluded
 461 because our focus was on remote sensing from satellites or airborne platforms. The final subset was read
 462 to analyze overarching trends in research focus and scale. Each of the resulting 236 papers was
 463 subsequently classified into one of the four categories outlined below.

- 464 1. *Purely methodological* – The purpose of the paper is to present and validate a new model or
 465 methodology. Results consist of model validation and error metrics. No figures depicting spatial
 466 or temporal patterns are present.
- 467 2. *Methodological with pattern analysis*: The paper is predominately methods development and validation
 468 but includes some figures applying the proposed model either spatially or temporally.
- 469 3. *Trend/pattern analysis*: The purpose of the paper is to examine spatiotemporal patterns and/or trends
 470 in water quality within the study area, with trends defined as having directionality over space or
 471 time. Model validation results are presented for transparency, but the bulk of the results and
 472 discussion focusses on either spatial or temporal trend analysis. The preponderance of figures and
 473 tables depict maps, time-series, or other spatiotemporal analyses.
- 474 4. *Water quality science research with a focus on impacts and drivers*: The paper contains specific hypotheses
 475 and/or science questions to be directly addressed. Results and discussion focus on spatiotemporal
 476 dynamics of water quality as well as the drivers and/or impacts of changing water quality. The
 477 preponderance of figures and tables present within the paper depict either trends or relationships
 478 between the parameter of interest and associated drivers/impacts.

479 Key questions that determined the classification of the papers included:

- 480 1. Is there a specific hypothesis or science question addressed?
- 481 2. Is there any spatial or temporal analysis of patterns or trends in the study area?
- 482 3. Are the majority of the figures and tables focused on validating a proposed model, or are they
 483 examining trends, drivers, and impacts of inland water quality?

484 With regards to the third criterion, figures and tables within each paper were categorized into the four
 485 groups depending on whether they provided background information, model validation, or
 486 spatiotemporal analysis (details in Table S1). The final index (Appendix A) depicts a field of research that
 487 has evolved, particularly in the last decade, from almost universally methods-focused into one in which
 488 new methodologies, data products, and increased computing power are creating opportunities to address
 489 science questions related to water quality in novel ways.

490 The overall trend in the publication counts of the detailed dataset closely parallels the power-law trend
 491 in the broad Scopus query, including a comparable spike in publications after 2008. Similarly, 75% of the
 492 studies resulting from the various searches focus on lakes and lake related water quality parameters (Figure

493 3). Eutrophication-associated parameters (chlorophyll, clarity, and cyanobacteria) are almost entirely
 494 measured in lake systems. In contrast, studies focusing on rivers, deltas, and estuaries are almost
 495 exclusively measuring sediment loading and transport parameters (TSS and turbidity).

496 In total, the included papers presented 411 models for constituent retrieval. Of these, only 70%
 497 reported some measure of goodness-of-fit or absolute error, and only 23% reported some measure of
 498 validation, with validation defined as an error metric derived from data not used in building the model.
 499 The most commonly reported metric was a coefficient of determination (R^2), with mean recorded values of

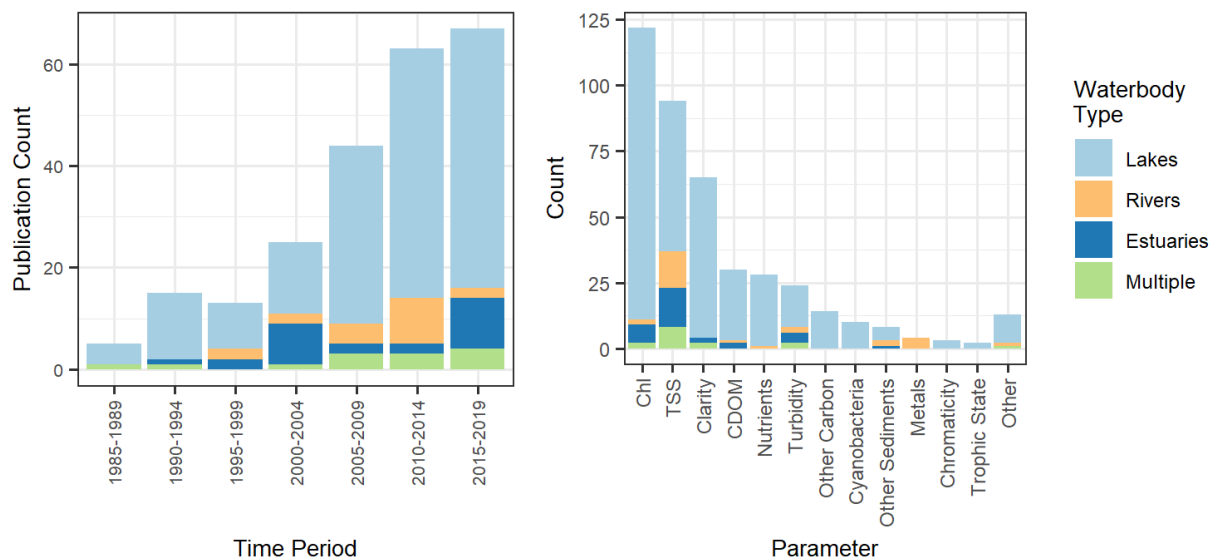


Figure 3. Publication counts within the detailed index binned by time and water quality parameter of interest. Colors represent type of waterbody being researched.

500 0.76 ($\sigma = 0.184$) for model fit and 0.79 ($\sigma = 0.159$) for model validation (Figure 4). Simple linear regression
 501 of R^2 values over time indicate that model
 502 fit has decreased ($p = 0.011$) and model
 503 validation has shown no significant trend
 504 ($p = 0.633$). However, more recent models
 505 frequently cover larger spatiotemporal
 506 domains and represent more difficult
 507 constituent retrieval, possibly leading to
 508 reduced model fit. While R^2 values are
 509 not the most robust stand-alone metric of
 510 model performance [215], comparisons
 511 utilizing other common metrics are
 512 difficult due to the lack of standardization
 513 between reported metrics within the
 514 reviewed publications. In total, over 35
 515 different error metrics were identified
 516 within the literature. Many of these
 517 represent differences in terminology as
 518 opposed to the actual statistical measure. For example, root mean square error (RMSE) is referred to nine
 519 different ways in total, with variations both in terminology (e.g. - root mean square error and root mean

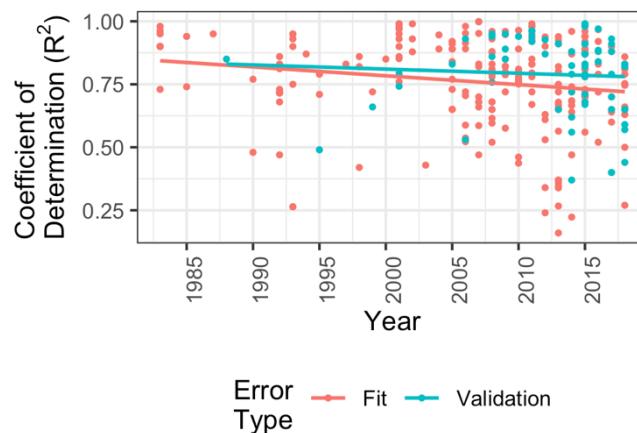


Figure 4. Reported R^2 values for model fit and model validation along with linear regressions of R^2 over time.

520 square deviation) and metric transformation (e.g. - percent, normalized, relative, and log values). Similar
 521 ranges of variation occur for mean/median absolute error (MAE), standard error (SE), relative error (RE),
 522 and bias. This disparity in reporting measures makes it difficult to accurately compare model error across
 523 studies without significant burden on the reader. However, examination of the most common metric, R^2 ,
 524 suggests consistently strong model fits dating back to the 1970s (Figure 4). These results suggest that the
 525 potential has long existed for remote sensing to contribute to addressing scientific questions related to
 526 water quality. The reasons for the lag between methods development and scientific application remain
 527 uncertain. Two possible explanations are that the empirical models that dominate early literature were too
 528 site-specific to be useful at larger scales, or that perceptions of the usefulness of remote sensing in water
 529 quality research differed between the remote sensing community and fields like hydrology, limnology, and
 530 ecology.

531 Trends in modelling approach indicate a fairly static field up until the early 1990s, with empirical
 532 modelling approaches comprising 50-80% of all publications for nearly 20 years (Figure 5). The mid-2000s
 533 show an increase in publications employing machine learning models and pre-produced satellite products.
 534 The emergence and subsequent decline of product-based studies from 2008-2015 likely corresponds to the

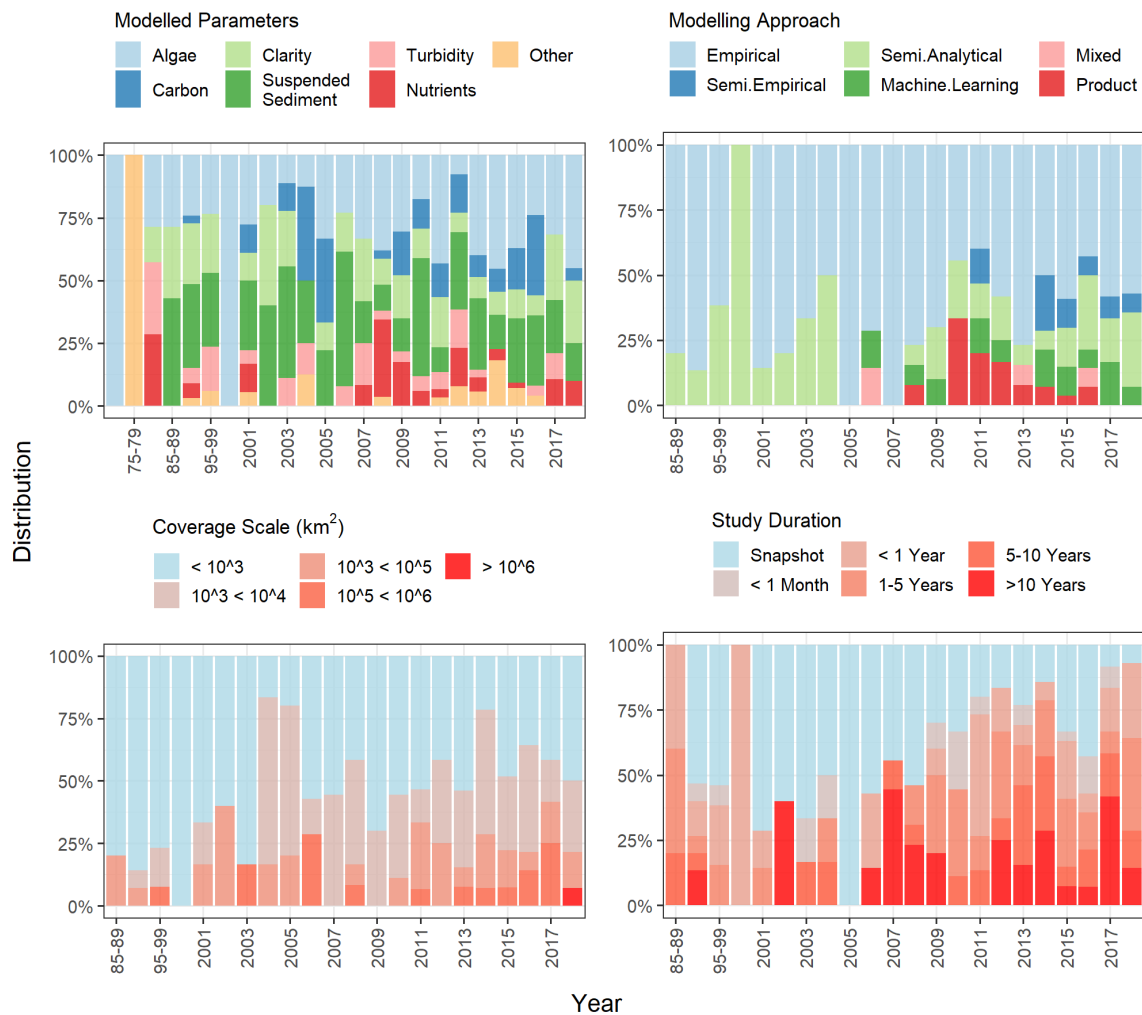


Figure 5. Temporal distributions of key study characteristics. Results for 1975-1999 are reported in five-year windows due to the relatively small number of studies published during this time period.

535 launch of the Medium Resolution Imaging Spectrometer (MERIS) in 2002 and its decommission in 2012.
536 MERIS presented a unique step towards global products through the development of the BEAM processing
537 toolbox (Brockman Consult in collaboration with the European Space Agency), which utilizes a neural
538 network scheme to simultaneously conduct atmospheric correction and water quality estimates. BEAM
539 provided ready-made water quality products to inland water and ocean researchers alike, though
540 validation of the products was regionally inconsistent [216–218].

541 The development of BEAM’s neural network scheme and the rise in machine learning approaches
542 starting around 2000 is likely attributable to increased computational capabilities and a proliferation of
543 specialized software in common programming environments like R and Python. For the former, packages
544 like Rpart [219], originally released in 1999, and nnet [220] created previously unavailable access to decision
545 tree and neural network modelling approaches. For Python, software development throughout the 2000s
546 led to comprehensive machine learning libraries such as Scikit-learn [221], which provided both access to
547 common machine learning algorithms and a framework for their calibration and validation. These
548 machine learning tools, among others, emerged in part due to an increased need for open source software
549 that promoted study replicability, researcher access, and collaborative code development for machine
550 learning researchers across fields [222].

551 The emergence of machine learning approaches in remote sensing of inland waters is paralleled by an
552 increase in semi-empirical models. Initially, this late appearance of semi-empirical models appears
553 unintuitive since they are computationally inexpensive and closely parallel older terrestrial indexes like
554 NDVI; however, their emergence is likely explained by a proliferation of data from ocean color sensors
555 such as SeaWiFs (launched 1997), MODIS Terra and Aqua (1999 and 2002 respectively), and MERIS (2002).
556 With MERIS specifically, its high spectral resolution and chlorophyll-specific band centers allowed for
557 better detection of absorption and backscattering peaks that facilitate semi-empirical models [88].
558 However, due to their coarse spatial resolution, these studies are mostly limited to larger lakes. These
559 sensors were subsequently joined by the hyperspectral sensor Hyperion in 2000, which created new
560 opportunities for semi-analytical water constituent retrieval [62].

561 Spatial examination of the literature reveals a dominance of studies located in the U.S., Europe, and
562 China (Figure 6). China and the U.S., respectively, comprise 20 and 24% of the total studies included, with
563 a notable clustering of long-term, large-scale studies in the Yangtze Basin. Spatiotemporal trends in
564 publication dates depict a temporal expansion outward, with the earliest studies located almost exclusively
565 in the U.S and subsequent publications spreading out across the globe. However, it should be noted that
566 this trend may be partially attributable to a language bias in early publications where there is less access to
567 non-English papers.

568 6. From methods to applications: an overview of inland water remote sensing

569 The study of water quality in lakes, rivers, and estuaries using remote sensing has expanded
570 substantially over the past 50 years. When considering the *intent* of the publications as opposed to just the
571 number, it is apparent that only in the past 10-15 years has inland water remote sensing consistently been
572 used as a powerful analytical tool informing the broader inland water literature. In the papers reviewed
573 for this analysis, twice as many studies were published in the past ten years as in the previous 28 years
574 combined, a rate much faster than the growth of academic publishing as a whole. Of papers published
575 since 2008, nearly 30% focus on examining drivers and impacts of water quality, compared to only 7% for
576 the period prior (Figure 7).

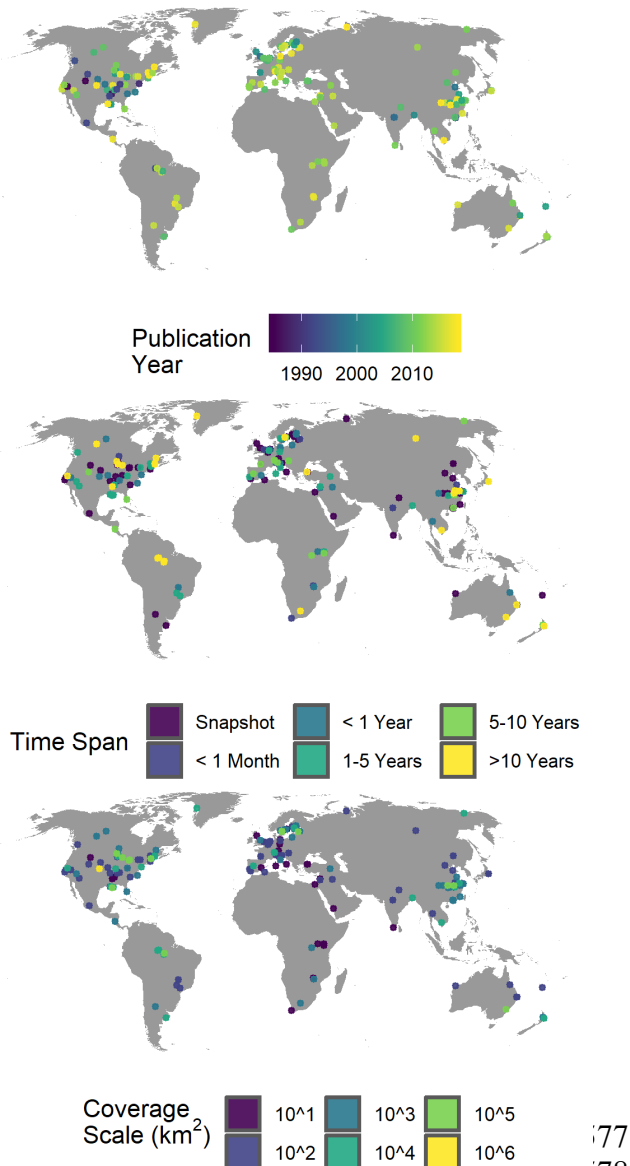


Figure 6. Spatial distribution of study publication date and scale

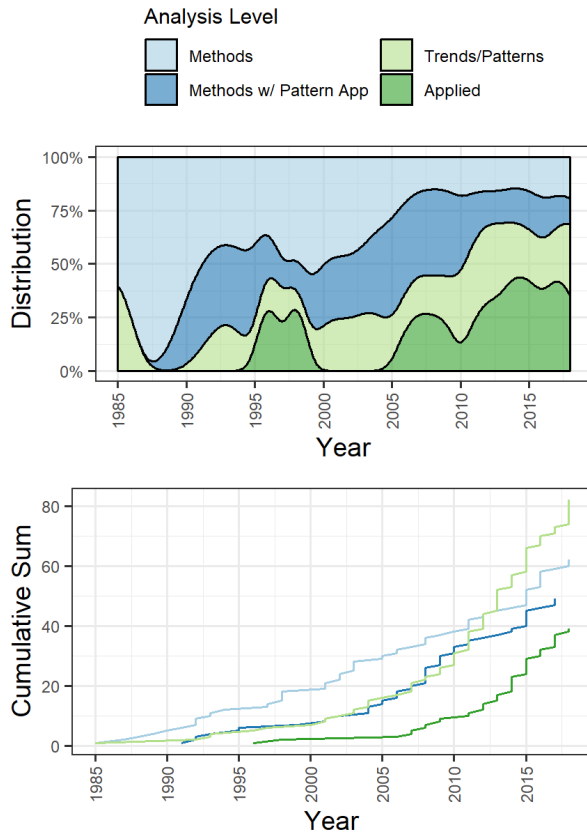


Figure 7: Progression of publication focus through time. Cumulative sum totals for methods categories (n = 113; 49%), trend/pattern papers (n = 81; 35%), and water quality science papers (n = 38;16%) show decreasing dominance of methods over time.

Studies are also expanding into longer time-frames and over larger spatial-scales (Figure 5). Pre-2008, the average study covered tens of square kilometers over a 2-year period. Post-2008, the average study examines hundreds of square

582 kilometers over a period of 5 years. This expansion requires the caveat that study scale is used as a proxy
 583 for the number of distinct lakes, and some of the increase in study scale may result from an increase in the
 584 average lake size rather than the total number of optically unique waterbodies. Similarly, longer term
 585 studies largely focus on simpler metrics such as water clarity and TSS, in part due to ongoing challenges
 586 modelling the more complex spectral signatures of chl-a and CDOM given the limited radiometric
 587 resolution of satellites like Landsat that provide longer time series of observations. Pearson's Correlation
 588 Coefficients [223] were calculated to identify relationships between study scale, duration, publishing date,
 589 and category. The category variable was converted to a numeric (1-4) in order of level of analysis (1,
 590 methods development; 2, methods with pattern analysis; 3, trend/pattern analysis; 4, water quality science).
 591 While the categorical classification of the included papers is partially subjective, their correlations with
 592 other study parameters are still included to provide insight into how the scientific application of

593 publications has changed with study scale and duration. The resulting correlation matrix (Table 2) depicts
 594 a clear pattern between study scale and impact over time. All four of the included variables were
 595 positively correlated at a 99% significance level (with the exception of study category and scale, $p=0.014$).
 596 While none of the correlations are particularly strong, their significance and consistency indicate that
 597 studies published later
 598 tend to cover larger
 599 spatiotemporal domains
 600 and focus more on
 601 analyzing water quality
 602 dynamics and impacts
 603 than on methods
 604 development.

Table 2. Correlation matrix of key study parameters. All correlation are significant at a 99% confidence interval (***). Study category rescaled to 1-4 representing the four levels of analysis from purely methodological to water quality science papers.

	Pub. Year	Study Duration	Study Scale	Study Category
Pub. Year	1	0.171	0.255	0.342
Study Duration	***	1	0.326	0.32
Study Scale	***	***	1	0.173
Study Category	***	***	***	1

605 This shift in study
 606 focus, scale, and duration all
 607 suggest that remote sensing

608 is becoming a useful tool in understanding inland water quality rather than an area for methodological
 609 study among remote sensing specialists. Publications representative of this shift towards hypothesis-
 610 driven science vary significantly in their focus, with emphasis on hydrological processes, drivers of water
 611 quality, public hazard identification, and impacts of degraded water quality (Table S2).

612 Studies examining drivers of water quality at local to regional scales comprise the largest group of
 613 water quality science publications. Recent work has examined climatic, anthropogenic, and landscape-
 614 scale variables that interact with complex biogeophysical water quality properties. Work by Lymburner
 615 et al. (2016)[175] presents a 30-year analysis of TSS in Australian lakes, showing distinct relationships
 616 between El Niño Southern Oscillations and fluctuations in TSS levels. Olmanson, Brezonik, & Bauer
 617 (2014)[224], examined a 20-year record of remotely sensed water clarity for over 10,000 lakes in Minnesota.
 618 Their results showed significant differences in overall trends based on land use and eco-region. Ng et al.
 619 (2011)[225] and Curtarelli et al. (2015)[98] both incorporated remotely sensed chl-a data into hydrologic
 620 models and found that thermal stratification and mixing were key drivers of algal bloom growth and
 621 dispersion. Work done by Rose et al. (2017)[148] showed that controls on water clarity move from local
 622 to watershed scales during dry and wet years respectively. Other studies focusing on climatic drivers of
 623 water quality have used remote sensing to analyze the impacts of hurricanes [226], typhoons [227], and
 624 growing season length [228] on various water quality metrics.

625 Studies focusing on anthropogenic drivers have brought to light the impacts of human activities on
 626 freshwater resources for areas ranging from individual lakes to entire states. Work by Cui and others (2009,
 627 2013)[229,230] examined the combined effects of precipitation, river flows, and dredging on TSS levels in
 628 Poyang Lake in China. They found that the combined precipitation and anthropogenic impacts degraded
 629 water quality far more than either individual driver could on its own. At a basin scale, Ren et al.
 630 (2018)[231] and Hou et al. (2017)[232] conducted studies examining how the Three Gorges Reservoir
 631 affected water clarity and TSS dynamics in the Yangtze Basin. In the Peace-Athabasca Delta, Pavelsky &
 632 Smith (2009)[233] and Long & Pavelsky (2013)[234] utilized multi-temporal images of sediment loads to
 633 calculate river velocity and recharge for floodplain lakes.

634 Studies using remote sensing of water quality to address scientific questions extend beyond the field
 635 of hydrology and into biology and public health. Sandström et al. (2016) [235] utilized remotely sensed
 636 CDOM and chl-a concentrations to analyze fish habitat assemblages and biodiversity. For public health,
 637 inland water remote sensing is helping to analyze disease distribution and drinking water hazards. Fichot
 638 et al. (2016)[70] identified spatial patterns of methylmercury in the San Francisco Bay area using an airplane

639 mounted hyperspectral sensor. Qin et al. (2015)[29] developed a dynamic forecasting model capable of
 640 predicting the presence of toxic algal blooms. The model ultimately resulted in over one million tons of
 641 algal scum being removed from a drinking water reservoir in China [29]. Other authors have similarly
 642 identified public threats to drinking water in Lake Mead (USA) [182] and Lake Chaohu in China [190].
 643 Two specific studies stood out through their novel use of remote sensing to facilitate epidemiological
 644 studies. Torbick et al. (2014)[236] incorporated Landsat-derived water quality parameters into an eco-
 645 epidemiological model to examine the distribution of amyotrophic lateral sclerosis (ALS) across New
 646 England. They found that close proximity to waterbodies with elevated levels of nitrogen increased the
 647 odds of being located within an ALS hotspot by 167%. Similarly, Finger et al. (2014)[237] incorporated
 648 remotely sensed chl-a measurements into a model of cholera dynamics within the Democratic Republic of
 649 Congo.

650 One additional subset of the reviewed literature merits discussion when considering advances in the
 651 field; specifically, researchers who are continuing to expand the spatiotemporal scale of their study areas.
 652 The need for global data products has received increasing attention in recent years as an essential aspect to
 653 protecting threatened freshwater resources [15–17]. Within the U.S., work towards this goal includes
 654 state-wide analyzes of Secchi Disk depth in Minnesota [157,224] and Maine [238], and a national approach
 655 to modelling lake chl-a [188]. Outside the U.S., previously mentioned work by Lymberner et al.
 656 (2016)[175] in Australian lakes and Hou et al. (2017)[232] in the Yangtze basin both cover areas of tens of
 657 thousands of square kilometers, albeit without including every lake in the study region.

658 Publications like those mentioned above are complemented by a host of living databases and
 659 interactive web services that are increasing access to near real-time water quality information. The
 660 Copernicus Inland Water Service provides semi-continuous (2002-2012, 2016-present) turbidity and chl-a
 661 observations for approximately 1,000 of the world's largest lakes
 662 (<https://land.copernicus.eu/global/products/lwq>). Similarly, the Minnesota LakeBrowser provides
 663 periodic measurements of chl-a, CDOM, and water clarity dating back to 2002 for over 10,000 lakes across
 664 the state (<https://lakes.rs.umn.edu/>). These publicly available databases are being supplemented by
 665 private companies like EOMAP (<https://www.eomap.com/>) which provide remotely sensed estimates of
 666 water quality parameters on a contract basis around the globe. While validation of some of these products
 667 is difficult to obtain, they are facilitating increased access to water quality data for water managers and
 668 researchers alike. Improvements in modeling methodologies and growing access to both *in situ* and earth
 669 observation data are setting the stage for future studies at larger and larger scales.

670 7. Emerging Trends in the Remote Sensing of Water Quality

671 The past decade has seen a dramatic growth in the resources necessary to remotely sense inland water
 672 quality. One example highlighted here is the 2008 shift to open access Landsat data, after which
 673 publication counts rose and study scale and duration increased significantly. However, the Landsat
 674 archive is only one of numerous petabyte-size archives of earth observation data provided by government
 675 agencies such as NASA, the USGS, NOAA, and the European Space Agency. These archives are
 676 constantly expanding and will continue to do so in the coming years. Starting in 2010, access to these data
 677 sources further increased with the release of the Google Earth Engine platform, which hosts imagery and
 678 resulting data products from over a dozen different earth observation sensors. The platform provides free
 679 access to these datasets along with cloud-based processing, dramatically increasing the computational
 680 power of remote sensing researchers across fields. For inland water remote sensing, Lin et al. (2018)[188]
 681 combined *in situ* data from the 2007 National Lake Assessment (N = 1157 lakes) with Landsat data and
 682 machine learning algorithms built into Earth Engine to develop a well-validated national model for lake
 683 chl-a (RMSE = 34.9 $\mu\text{g/L}$). Similarly, Overeem et al. (2017)[112] used Google Earth Engine to model

684 sediment export from Greenland over 14 years. Today, the platform continues to grow and increase in
685 usefulness, adding approximately 6,000 scenes daily from various active satellite missions, with a latency
686 of approximately 24 hours [239]. The power of Google Earth Engine essentially provides researchers with
687 supercomputing capabilities from their local machines, dramatically increasing the scales at which earth
688 observation research can take place. Platforms like Earth Engine are complimented by an ever-growing
689 body of processing and analysis software in common programming languages like R [240].

690 While the provision of open-access satellite imagery to researchers is essential to the progression of
691 the field, it alone cannot account for the shift in research focus and scale outlined above. Paralleling the
692 rise in remote sensing data availability over the past decade has been a rise in the *in situ* data available for
693 model calibration and validation. In the past, the burden of collecting this data frequently fell on
694 individual researchers, significantly limiting the amount of field data available. Recent databases
695 provided by government agencies, NGOs, and researchers alike are providing a wealth of freely available
696 *in situ* data that is easily accessible. At a global level, the GEMStat database maintained through the
697 International Centre for Water Resources and Global Change, provides over 4 million observations of lakes,
698 rivers, wetlands, and groundwater systems from 4,000 sites spread over 75 countries (<https://gemstat.org/>).
699 In the U.S., The National Water Quality Portal (WQP), released in 2012 by the USGS, EPA, and National
700 Water Quality Monitoring Network, provides national coverage of archived state, federal, and tribal water
701 quality field measurements. In total it assimilates and standardizes monitoring data for over 2 million
702 individual sampling sites [241]. The Lake Multi-Scaled Geospatial and Temporal Database (LAGOS-NE)
703 provides a similar assimilation of *in situ* water quality measurements for 17 water-rich states in the upper
704 Midwest and Northeast United States, providing historical field data for over 51,000 lakes and reservoirs
705 [242]. These datasets have already been used as calibration and validation data for remote sensing of
706 water skin temperature [243]. In Europe, national-scale water quality data for inland and coastal waters
707 are compiled from participating agencies into the Waterbase dataset, which is harmonized and made
708 research ready under the WISE system (water information system for Europe) [244]. These official data
709 sources can be supplemented with novel collections aggregated through citizen science campaigns. These
710 include Eye On Water (<http://www.eyeonwater.org/>) and Seen-monitoring (<http://www.seen-transparent.de/>)
711 in Europe, the Secchi-Dip In in North America (<http://www.secchidipin.org/>), and state
712 level efforts in Minnesota, Wisconsin, Michigan, and Maine ([https://www.pca.state.mn.us/water/citizen-](https://www.pca.state.mn.us/water/citizen-water-monitoring)
713 [water-monitoring,](https://www.uwsp.edu/cnr-ap/UWEXLakes/Pages/programs/clmn/default.aspx) [https://www.uwsp.edu/cnr-ap/UWEXLakes/Pages/programs/clmn/default.aspx,](https://www.uwsp.edu/cnr-ap/UWEXLakes/Pages/programs/clmn/default.aspx)
714 <https://micorps.net/lake-monitoring/>, and <https://www.lakestewardsofmaine.org/> respectively). Together
715 these campaigns have collected hundreds of thousands of observations available to researchers. The new
716 AquaSat database from Ross et al. (*in review*) [245] uses Google Earth Engine to extract coincident (+/- 1 day)
717 Landsat reflectance values for *in situ* measurements found in the WQP and LAGOS-NE. The result is the
718 first dataset of its kind, providing over 500,000 paired observations of reflectance values and associated
719 water quality parameters in optically complex waters dating back to 1984. Databases such as these
720 provide data continuity, cost and time savings for researchers, and large calibration and validation samples
721 for model development.

722 The development and expansion of new and existing databases is paralleled by the development of
723 new sensor technology. Airborne hyperspectral sensors capable of capturing contiguous spectral
724 signatures of water-leaving radiance have provided new levels of precision to measure optically active
725 constituents (see reviews by [3,60]). These airborne campaigns are working towards satellite missions
726 such as NASA's Surface Biology and Geology mission (SBG, in development), Italy's PRecursores
727 IperSpettrale della Missione Applicativa (PRISMA, launched March 22, 2019), Japan's Hyperspectral
728 Imaging Suite (HISUI, planned 2019), and Germany's Environmental Mapping and Analysis Program
729 (EnMAP, planned 2020) [246]. These spaceborne imaging spectrometers will increase spatiotemporal
730 transferability of retrieval models, improve overall constituent retrieval, facilitate biogeochemical

731 composition analysis, enable benthic habitat identification in optically shallow water bodies, and allow for
 732 the retrieval of additional detectable water quality parameters that are currently unfeasible with
 733 broadband, multispectral sensors, all while providing global hyperspectral data at roughly 30 meter
 734 resolution [17,18]. Traditional governmental satellite missions are being supplemented with a host of
 735 novel earth observation technologies being developed by commercial companies such as Planet
 736 (<https://www.planet.com/>), MAXAR (<https://www.maxar.com/>), and Airbus (<https://www.airbus.com/>).
 737 These private platforms are creating novel opportunities for hydrological remote sensing through public
 738 and academic research partnerships. For example, Planet, which operates over 150 small imaging
 739 satellites that provide daily global imagery at 3-5 meter resolution, collaborated with Cooley et al.
 740 (2017)[247] to study lake connectivity in the Yukon Flats region of Alaska at previously unfeasible spatial
 741 scales. For inland water quality, the high spatial and temporal resolution of such satellite constellations
 742 will allow for detection of short-term phenomena like algal blooms in streams and lakes that are currently
 743 too small to study with publicly available satellite imagery. These efforts to improve research in small
 744 aquatic systems are being further aided by the increased use of unmanned aerial vehicles and even
 745 smartphones [248].

746 These emerging technologies will allow the inland water quality remote sensing community to
 747 overcome historic challenges and examine new science questions. However, this process will require
 748 dedicated researchers and reliable funding sources. While emerging technologies hold promise, they also
 749 present new challenges. Hyperion, the first spaceborne hyperspectral sensor believed to be appropriate
 750 for inland waters, showed initial promise [62] but ultimately proved unreliable over waterbodies due to its
 751 low signal to noise ratio and radiometric instability [249]. The Planet constellation of CubeSats, while
 752 providing unprecedented spatial and temporal resolution, are subject to geolocation accuracy errors and
 753 inconsistencies in radiometric calibration between satellites [247]. These issues are in addition to well-
 754 characterized challenges including robust atmospheric correction and solving adjacency effects, both of
 755 which need to be applied across sensors to create comparable datasets. Solutions to these existing
 756 challenges will likely be developed through improvements in sensor engineering, computational capacity,
 757 and modelling approaches, as well as growing collaborative efforts by international groups such as IOCCG
 758 [20,250] and the Committee on Earth Observation Satellites [56]. As existing issues are overcome, remote
 759 sensing of inland water quality can be applied to address relevant scientific questions and conservation
 760 goals, including those outlined in the NRC Decadal Survey [251] and the EU Water Framework Directive
 761 [252]. Conducting such research will help solve water quality issues of global importance and better
 762 inform water managers, policy makers, and the scientific community regarding critical science questions.
 763 Some of the most pressing questions synthesized from the reviewed literature include:

- 764 • How does biogeochemical cycling of suspended sediments and CDOM in lakes and rivers contribute
 765 to the global carbon cycle?
- 766 • How are added nutrient inputs and warming air temperatures contributing to the frequency and
 767 distribution of harmful algal blooms in lakes and reservoirs?
- 768 • What is the impact of anthropogenic development, including urbanization and reservoir construction,
 769 on basin-wide water quality?
- 770 • What are the patterns and trends in the biogeochemistry of water resources in remote, vulnerable areas
 771 including the Arctic and Boreal regions?
- 772 • How are changes in water quality affecting the biological structure of freshwater resources at regional
 773 to global scales?
- 774 • How are changing water quality dynamics impacting important drinking water resources?

775 8. Conclusion

776 The bibliometric analysis presented here highlights the dramatic growth of inland water quality
777 remote sensing studies, far outpacing the average rate of increase in academic publishing as a whole. The
778 past 50 years have produced hundreds of remote sensing publications accurately estimating
779 biogeochemical water quality parameters; however, the majority of these focus on methods development
780 rather than using remote sensing as a tool to better understand inland water quality dynamics. Detailed
781 examination of 236 of the most relevant publications returned by search queries indicates that the past 10-
782 15 years has brought about a focal shift within the field, where researchers are moving beyond methods
783 development towards research focused on spatiotemporally explicit water quality dynamics. This shift is
784 partially attributable to the development of new satellite and *in situ* datasets, improved access to satellite
785 imagery, and increased computational/software capabilities. The current change in focus within the field
786 is similar in nature to the shift that occurred in ocean color and terrestrial remote sensing throughout the
787 1980s and 1990s, after which time both fields applied remote sensing to answer some of the most pressing
788 science questions of their time. For inland water quality, the progression of research is evidenced by a
789 subset of recent publications which have begun to leverage remote sensing to examine water quality trends,
790 ecological and anthropogenic drivers, and resulting impacts of changing water quality on ecosystem
791 function and water resources. This shift has been accompanied by a significant increase in the
792 spatiotemporal scale of analysis, moving the field closer to providing national to global-scale data products
793 for policy makers, water managers, and scientists. The increase in high quality science and study scale
794 within the field continues to be facilitated by improved data-sets and growing computational
795 capacity. New data products like AquaSat [245] promise to continue this trajectory of growth and facilitate
796 a new generation of inland water remote sensing research.

797 Based on the literature reviewed here, future inland water quality remote sensing work will benefit
798 greatly from the following recommendations: 1) continued development of generalizable constituent
799 retrieval models, including atmospheric corrections, that are applicable across large spatiotemporal
800 domains and across differing sensors; 2) the expanded application of robust, generalizable models to better
801 understand global processes including erosion and deposition, terrestrial carbon and nutrient cycling, and
802 trends in algal bloom dynamics in inland waters ; 3) improved communication between experts in remote
803 sensing and scientists in fields such as hydrology, limnology, and ecology, in order to facilitate the wider
804 adoption of remote sensing models in scientific studies of water quality; and, 4) the development of user-
805 friendly tools that inform local water managers of remotely sensed changes in water quality to promote
806 sound policy and the conservation of essential freshwater resources.

807 **References**

- 808 1. Wrigley, R.C.; Horne, A.J. Remote sensing and lake eutrophication. *Nature* **1974**, *250*, 213–214.
- 809 2. Scarpace, F.; Holmquist, K.; Fisher, L. Landsat analysis of lake quality. *Photogramm. Eng. Remote Sensing* **1979**,
810 *45*, 623–633.
- 811 3. Gholizadeh, M.; Melesse, A.; Reddi, L. A Comprehensive Review on Water Quality Parameters Estimation
812 Using Remote Sensing Techniques. *Sensors* **2016**, *16*, 1298.
- 813 4. Matthews, M.W. A current review of empirical procedures of remote sensing in Inland and near-coastal
814 transitional waters. *Int. J. Remote Sens.* **2011**, *32*, 6855–6899.
- 815 5. Odermatt, D.; Gitelson, A.; Brando, V.E.; Schaepman, M. Review of constituent retrieval in optically deep and
816 complex waters from satellite imagery. *Remote Sens. Environ.* **2012**, *118*, 116–126.
- 817 6. Liu, Y.S.; Islam, M.A.; Gao, J. Quantification of shallow water quality parameters by means of remote sensing .
818 *Prog. Phys. Geogr.* **2003**, *27*, 24–43.
- 819 7. Tucker, C.J. Red and photographic infrared linear combinations for monitoring vegetation. *Remote Sens. Environ.*
820 **1979**, *8*, 127–150.
- 821 8. Matthews, E. Global Vegetation and Land Use: New High-Resolution Data Bases for Climate Studies. *J. Clim.*
822 *Appl. Meteorol.* **1983**, *22*, 474–487.
- 823 9. Tarpley, J.D.; Schneider, S.R.; Money, R.L. Global Vegetation Indices from the NOAA-7 Meteorological Satellite.
824 *J. Clim. Appl. Meteorology* **1984**, *23*, 491–494.
- 825 10. Box, E.O.; Holben, B.N.; Kalb, V. Accuracy of the AVHRR vegetation index as a predictor of biomass, primary
826 productivity and net CO₂ flux. *Vegetatio* **1989**, *80*, 71–89.
- 827 11. Tucker, C.J.; Fung, I.Y.; Keeling, C.D.; Gammon, R.H. Relationship between atmospheric CO₂ variations and a
828 satellite-derived vegetation index. *Nature* **1986**, *319*, 195–199.
- 829 12. Feldman, G.; Kuring, N.; Ng, C.; Esaias, W.; McClain, C.; Elrod, J.; Maynard, N.; Endres, D.; Evans, R.; Brown,
830 J.; et al. Ocean color: Availability of the global data set. *Eos, Trans. Am. Geophys. Union* **1989**, *70*, 634.
- 831 13. Platt, T.; Sathyendranath, S. Oceanic Remote Primary Production: Estimation by Remote Sensing at Local and
832 Regional Scales. *Science (80-.)*. **1988**, *241*, 1613–1620.
- 833 14. Zandaryaa, S. *The UNESCO-IHP IIWQ World Water Quality Portal - Whitepaper -*; 2018;
- 834 15. Lee, B.Z.; Arnone, R.; Boyce, D.; Franz, B.; Greb, S.; Hu, C.; Lewis, M.; Schaeffer, B.; Shang, S.; Wang, M.; et al.
835 Global Water Clarity : Continuing a Century-Long Monitoring. *Eos (Washington. DC)*. **2018**, *99*, 1–10.
- 836 16. Malthus, T.J.; Hestir, E.L.; Dekker, A.G.; Brando, V.E. The case for a global inland water quality product. *IEEE*
837 *IGARSS* **2012**, 5234–5237.
- 838 17. Hestir, E.L.; Brando, V.E.; Bresciani, M.; Giardino, C.; Matta, E.; Villa, P.; Dekker, A.G. Measuring freshwater
839 aquatic ecosystems: The need for a hyperspectral global mapping satellite mission. *Remote Sens. Environ.* **2015**,
840 *167*, 181–195.
- 841 18. Giardino, C.; Brando, V.E.; Gege, P.; Pinnel, N.; Hochberg, E.; Knaeps, E.; Reusen, I.; Doerffer, R.; Bresciani, M.;
842 Braga, F.; et al. Imaging Spectrometry of Inland and Coastal Waters : State of the Art , Achievements and
843 Perspectives. *Surv. Geophys.* **2019**, *40*, 401–429.
- 844 19. Tyler, A.N.; Hunter, P.D.; Spyrakos, E.; Groom, S.; Constantinescu, A.M.; Kitchen, J. Developments in Earth
845 observation for the assessment and monitoring of inland, transitional, coastal and shelf-sea waters. *Sci. Total*
846 *Environ.* **2016**, *572*, 1307–1321.
- 847 20. IOCCG. Earth Observations in Support of Global Water Quality Monitoring. Greb, S., Dekker, A.
848 and Binding, C. (eds.), IOCCG Report Series, No. 17, International Ocean Colour Coordinating Group,
849 Dartmouth, Canada, **2018**;
- 850 21. Bukata, R.P.; Bruton, J.E.; Jerome, J.H.; Jain, S.C.; Zwick, H.H. Optical water quality model of Lake Ontario 2:
851 Determination of chlorophyll a and suspended mineral concentrations of natural waters from submersible and
852 low altitude optical sensors. *Appl. Opt.* **1981**, *20*, 1704.
- 853 22. Bukata, R.P.; Jerome, J.H.; Bruton, J.E. Particulate concentrations in Lake St. Clair as recorded by a shipborne
854 multispectral optical monitoring system. *Remote Sens. Environ.* **1988**, *25*, 201–229.
- 855 23. Dekker, A.G.; Seyhan, E. The remote sensing loosdrecht lakes project. *Int. J. Remote Sens.* **1988**, *9*, 1761–1773.
- 856 24. Kirk, J.T.O.; Tyler, P.A. The spectral absorption and scattering properties of dissolved and particulate
857 components in relation to the underwater light field of some tropical Australian fresh waters. *Freshw. Biol.* **1986**,

- 858 16, 573–583.
- 859 25. Kishino, M.; Booth, C.R.; Okami, N. Underwater radiant energy absorbed by phytoplankton, detritus, dissolved
860 organic matter, and pure water. *Limnol. Oceanogr.* **1984**, *29*, 340–349.
- 861 26. Seyhan, E.; Dekker, A. Application of Remote Sensing Techniques for Water Quality Monitoring. *Hydrobiol. Bull.*
862 **1986**, *20*, 41–50.
- 863 27. Stumpf, R.P.; Pennock, J.R. Calibration of a general optical equation for remote sensing of suspended sediments
864 in a moderately turbid estuary. *J. Geophys. Res.* **1989**, *94*, 14363.
- 865 28. Walker, N.D. Satellite assessment of Mississippi River plume variability: Causes and predictability. *Remote Sens.*
866 *Environ.* **1996**, *58*, 21–35.
- 867 29. Qin, B.; Li, W.; Zhu, G.; Zhang, Y.; Wu, T.; Gao, G. Cyanobacterial bloom management through integrated
868 monitoring and forecasting in large shallow eutrophic Lake Taihu (China). *J. Hazard. Mater.* **2015**, *287*, 356–363.
- 869 30. Falcini, F.; Khan, N.S.; Macelloni, L.; Horton, B.P.; Lutken, C.B.; Mckee, K.L.; Santoleri, R.; Colella, S.; Li, C.;
870 Volpe, G.; et al. Linking the historic 2011 Mississippi River flood to coastal wetland sedimentation. *Nat. Geosci.*
871 **2012**, *5*, 803–807.
- 872 31. Miller, R.L.; McKee, B.A. Using MODIS Terra 250 m imagery to map concentrations of total suspended matter
873 in coastal waters. *Remote Sens. Environ.* **2004**, *93*, 259–266.
- 874 32. Adamo, M.; Matta, E.; Bresciani, M.; Carolis, G. De; Vaiciute, D.; Giardino, C.; Pasquariello, G. On the synergistic
875 use of SAR and optical imagery to monitor cyanobacteria blooms: The Curonian Lagoon case study. *Eur. J.*
876 *Remote Sens.* **2013**, *46*, 789–805.
- 877 33. Matthews, M.W.; Bernard, S.; Winter, K. Remote sensing of cyanobacteria-dominant algal blooms and water
878 quality parameters in Zeekoevlei, a small hypertrophic lake, using MERIS. *Remote Sens. Environ.* **2010**, *114*, 2070–
879 2087.
- 880 34. Palmer, S.C.J.; Odermatt, D.; Hunter, P.D.; Brockmann, C.; Présing, M.; Balzter, H.; Tóth, V.R. Satellite remote
881 sensing of phytoplankton phenology in Lake Balaton using 10 years of MERIS observations. *Remote Sens. Environ.*
882 **2015**, *158*, 441–452.
- 883 35. Bresciani, M.; Stroppiana, D.; Odermatt, D.; Morabito, G.; Giardino, C. Assessing remotely sensed chlorophyll-
884 a for the implementation of the Water Framework Directive in European perialpine lakes. *Sci. Total Environ.*
885 **2011**, *409*, 3083–3091.
- 886 36. Bresciani, M.; Vascellari, M.; Giardino, C.; Matta, E. Remote sensing supports the definition of the water quality
887 status of Lake Omodeo (Italy). *Eur. J. Remote Sens.* **2012**, *45*, 349–360.
- 888 37. Shen, M.; Duan, H.; Cao, Z.; Xue, K.; Loisel, S.; Yesou, H. Determination of the downwelling diffuse
889 attenuation coefficient of lakewater with the sentinel-3A OLCI. *Remote Sens.* **2017**, *9*.
- 890 38. Ritchie, J.C.; Cooper, C.M.; Schiebe, F.R. The relationship of MSS and TM digital data with suspended sediments,
891 chlorophyll, and temperature in Moon Lake, Mississippi. *Remote Sens. Environ.* **1990**, *33*, 137–148.
- 892 39. Kloiber, S.M.; Brezonik, P.L.; Bauer, M.E. Application of Landsat imagery to regional-scale assessments of lake
893 clarity. *Water Res.* **2002**, *36*, 4330–4340.
- 894 40. Mertes, L.A.K.; Smith, M.O.; Adams, J.B. Estimating suspended sediment concentrations in surface waters of
895 the Amazon River wetlands from Landsat images. *Remote Sens. Environ.* **1993**, *43*, 281–301.
- 896 41. Wang, Y.; Xia, H.; Fu, J.; Sheng, G. Water quality change in reservoirs of Shenzhen, China: detection using
897 LANDSAT/TM data. *Sci. Total Environ.* **2004**, *328*, 195–206.
- 898 42. Dekker, A.G.; Peters, S.W.M. The use of the thematic mapper for the analysis of eutrophic lakes: A case study
899 in the Netherlands. *Int. J. Remote Sens.* **1993**, *14*, 799–821.
- 900 43. Yacobi, Y.Z.; Gitelson, A.; Mayo, M. Remote sensing of chlorophyll in Lake Kinneret using high spectral
901 resolution radiometer and Landsat Thematic Mapper Spectral features of reflectance and algorithm
902 development. *J. Plankton Res.* **1995**, *17*, 2155–2173.
- 903 44. Ouillon, S.; Douillet, P.; Andréfouët, S. Coupling satellite data with in situ measurements and numerical
904 modeling to study fine suspended-sediment transport: A study for the lagoon of New Caledonia. *Coral Reefs*
905 **2004**, *23*, 109–122.
- 906 45. Tyler, A.N.; Svab, E.; Preston, T.; Présing, M.; Kovács, W.A. Remote sensing of the water quality of shallow
907 lakes: A mixture modelling approach to quantifying phytoplankton in water characterized by high-suspended
908 sediment. *Int. J. Remote Sens.* **2006**, *27*, 1521–1537.
- 909 46. Duan, H.; Zhang, Y.; Zhang, B.; Song, K.; Wang, Z. Assessment of chlorophyll-a concentration and trophic state
910 for lake Chagan using Landsat TM and field spectral data. *Environ. Monit. Assess.* **2007**, *129*, 295–308.

- 911 47. Watanabe, F.S.Y.; Alcântara, E.; Rodrigues, T.W.P.; Imai, N.N.; Barbosa, C.C.F.; Rotta, L.H. da S. Estimation of
912 chlorophyll-a concentration and the trophic state of the barra bonita hydroelectric reservoir using OLI/landsat-
913 8 images. *Int. J. Environ. Res. Public Health* **2015**, *12*, 10391–10417.
- 914 48. Lee, Z.; Shang, S.; Qi, L.; Yan, J.; Lin, G. A semi-analytical scheme to estimate Secchi-disk depth from Landsat-8
915 measurements. *Remote Sens. Environ.* **2016**, *177*, 101–106.
- 916 49. Toming, K.; Kutser, T.; Laas, A.; Sepp, M.; Paavel, B.; Nõges, T. First experiences in mapping lakewater quality
917 parameters with sentinel-2 MSI imagery. *Remote Sens.* **2016**, *8*, 1–14.
- 918 50. Kutser, T.; Paavel, B.; Verpoorter, C.; Ligi, M.; Soomets, T.; Toming, K.; Casal, G. Remote sensing of black lakes
919 and using 810 nm reflectance peak for retrieving water quality parameters of optically complex waters. *Remote*
920 *Sens.* **2016**, *8*.
- 921 51. Doxaran, D.; Froidefond, J.M.; Lavender, S.; Castaing, P. Spectral signature of highly turbid waters: Application
922 with SPOT data to quantify suspended particulate matter concentrations. *Remote Sens. Environ.* **2002**, *81*, 149–
923 161.
- 924 52. Dvornikov, Y.; Leibman, M.; Heim, B.; Bartsch, A.; Herzschuh, U.; Skorospekhova, T.; Fedorova, I.; Khomutov,
925 A.; Widhalm, B.; Gubarkov, A.; et al. Terrestrial CDOM in lakes of Yamal Peninsula: Connection to lake and
926 lake catchment properties. *Remote Sens.* **2018**, *10*, 1–21.
- 927 53. Hellweger, F.L.; Miller, W.; Oshodi, K.S. Mapping turbidity in the Charles River, Boston using a high-resolution
928 satellite. *Environ. Monit. Assess.* **2007**, *132*, 311–320.
- 929 54. Sawaya, K.; Olmanson, L.G.; Heinert, N.; Brezonik, P.; Bauer, M. Extending satellite remote sensing to local
930 scales: land and water resource monitoring using high-resolution imagery. *Remote Sens. Environ.* **2003**, *88*, 144–
931 156.
- 932 55. Olmanson, L.G.; Brezonik, P.L.; Bauer, M.E. Evaluation of medium to low resolution satellite imagery for
933 regional lake water quality assessments. *Water Resour. Res.* **2011**, *47*, 1–14.
- 934 56. CEOS *Feasibility Study for an Aquatic Ecosystem Earth Observing System*; Dekker, A.G., Pinnel, N., Eds.; 2018;
- 935 57. Buiteveld, H.; Hakvoort, J.H.M.; Donze, M. Optical properties of pure water. In *Proceedings of the Proceedings*
936 *of SPIE 2258*; Jaffe, J.S., Ed.; 1994; pp. 174–183.
- 937 58. Röttgers, R.; McKee, D.; Utschig, C. Temperature and salinity correction coefficients for light absorption by
938 water in the visible to infrared spectral region. *Opt. Express* **2014**, *22*, 25093.
- 939 59. IOCCG. Remote Sensing of Ocean Colour in Coastal, and Other Optically-Complex, Waters. Sathyendranath, S.
940 (ed.), *Reports of the International Ocean-Colour Coordinating Group*, No. 3, **2000**;
- 941 60. Govender, M.; Chetty, K.; Bulcock, H. A review of hyperspectral remote sensing and its application in vegetation
942 and water resource studies. *Water SA* **2007**, *33*, 145–151.
- 943 61. Bioucas-dias, J.M.; Plaza, A.; Camps-valls, G.; Scheunders, P.; Nasrabadi, N.M.; Chanussot, J. Hyperspectral
944 Remote Sensing Data Analysis and Future Challenges. *IEEE Geosci. Remote Sens. Mag.* **2013**, 6–36.
- 945 62. Brando, V.E.; Dekker, A.G. Satellite hyperspectral remote sensing for estimating estuarine and coastal water
946 quality. *IEEE Trans. Geosci. Remote Sens.* **2003**, *41*, 1378–1387.
- 947 63. Fang, L.; Chen, S.; Li, H.; Gu, C. Monitoring water constituents and salinity variations of saltwater using EO-1
948 Hyperion satellite imagery in the Pearl River Estuary, China. In *Proceedings of the IGARSS 2008 - 2008 IEEE*
949 *International Geoscience and Remote Sensing Symposium*; IEEE, 2008; Vol. 1, pp. I-438–I-441.
- 950 64. Hunter, P.D.; Tyler, A.N.; Willby, N.J.; Gilvear, D.J. The spatial dynamics of vertical migration by *Microcystis*
951 *aeruginosa* in a eutrophic shallow lake: A case study using high spatial resolution time-series airborne remote
952 sensing. *Limnol. Oceanogr.* **2008**, *53*, 2391–2406.
- 953 65. Wass, P.D.; Marks, S.D.; Finch, J.W.; Leeks, G.J.L.; Ingram, J.K. Monitoring and preliminary interpretation of in-
954 river turbidity and remote sensed imagery for suspended sediment transport studies in the Humber catchment.
955 *Sci. Total Environ.* **1997**, *194–195*, 263–283.
- 956 66. Knaeps, E.; Ruddick, K.G.; Doxaran, D.; Dogliotti, A.I.; Nechad, B.; Raymaekers, D.; Sterckx, S. A SWIR based
957 algorithm to retrieve total suspended matter in extremely turbid waters. *Remote Sens. Environ.* **2015**, *168*, 66–79.
- 958 67. Choe, E.; van der Meer, F.; van Ruitenbeek, F.; van der Werff, H.; de Smeth, B.; Kim, K.W. Mapping of heavy
959 metal pollution in stream sediments using combined geochemistry, field spectroscopy, and hyperspectral
960 remote sensing: A case study of the Rodalquilar mining area, SE Spain. *Remote Sens. Environ.* **2008**, *112*, 3222–
961 3233.
- 962 68. Palacios, S.L.; Kudela, R.M.; Guild, L.S.; Negrey, K.H.; Torres-Perez, J.; Broughton, J. Remote sensing of
963 phytoplankton functional types in the coastal ocean from the HypSPiRI Preparatory Flight Campaign. *Remote*

- 964 *Sens. Environ.* **2015**, *167*, 269–280.
- 965 69. Jensen, D.; Simard, M.; Cavanaugh, K.; Sheng, Y.; Fichot, C.G.; Pavelsky, T.; Twilley, R. Improving the
966 Transferability of Suspended Solid Estimation in Wetland and Deltaic Waters with an Empirical Hyperspectral
967 Approach.
- 968 70. Fichot, C.G.; Downing, B.D.; Bergamaschi, B.A.; Windham-Myers, L.; Marvin-Dipasquale, M.; Thompson, D.R.;
969 Gierach, M.M. High-Resolution Remote Sensing of Water Quality in the San Francisco Bay-Delta Estuary.
970 *Environ. Sci. Technol.* **2015**, *50*, 573–583.
- 971 71. Mobley, C.D. Light and Water : Radiative Transfer in Natural Waters. *Light Water Radiat. Transf. Nat. Waters*
972 **1994**, 592.
- 973 72. Morel, A.Y.; Gordon, H.R. Report of the working group on water color. *Boundary-Layer Meteorol.* **1980**, *18*, 343–
974 355.
- 975 73. McCullough, I.M.; Loftin, C.S.; Sader, S.A. Combining lake and watershed characteristics with Landsat TM data
976 for remote estimation of regional lake clarity. *Remote Sens. Environ.* **2012**, *123*, 109–115.
- 977 74. Torbick, N.; Hession, S.; Hagen, S.; Wiangwang, N.; Becker, B.; Qi, J. Mapping inland lake water quality across
978 the Lower Peninsula of Michigan using Landsat TM imagery. *Int. J. Remote Sens.* **2013**, *34*, 7607–7624.
- 979 75. Lillesand, T.M.; Johnson, W.L.; Deuell, R.L. Use of landsat data to predict the trophic state of Minnesota lakes.
980 *Photogramm. Eng. Remote Sensing* **1983**, *49*, 219–229.
- 981 76. He, W.; Chen, S.; Liu, X.; Chen, J. Water quality monitoring in a slightly-polluted inland water body through
982 remote sensing - Case study of the Guanting Reservoir in Beijing, China. *Front. Environ. Sci. Eng. China* **2008**, *2*,
983 163–171.
- 984 77. Choe, E.; van der Meer, F.; van Ruitenbeek, F.; van der Werff, H.; de Smeth, B.; Kim, K.W. Mapping of heavy
985 metal pollution in stream sediments using combined geochemistry, field spectroscopy, and hyperspectral
986 remote sensing: A case study of the Rodalquilar mining area, SE Spain. *Remote Sens. Environ.* **2008**, *112*, 3222–
987 3233.
- 988 78. Baban, S.M.J. Detecting water quality parameters in the norfolk broads, U.K., using landsat imagery. *Int. J.*
989 *Remote Sens.* **1993**, *14*, 1247–1267.
- 990 79. Kutser, T. Passive optical remote sensing of cyanobacteria and other intense phytoplankton blooms in coastal
991 and inland waters. *Int. J. Remote Sens.* **2009**, *30*, 4401–4425.
- 992 80. McCormick, P. V.; Cairns, J. Algae as indicators of environmental change. *J. Appl. Phycol.* **1994**, *6*, 509–526.
- 993 81. Carvalho, L.; Poikane, S.; Lyche Solheim, A.; Phillips, G.; Borics, G.; Catalan, J.; De Hoyos, C.; Drakare, S.;
994 Dudley, B.J.; Järvinen, M.; et al. Strength and uncertainty of phytoplankton metrics for assessing eutrophication
995 impacts in lakes. *Hydrobiologia* **2013**, *704*, 127–140.
- 996 82. Svirčev, Z.; Simeunović, J.; Subakov-Simić, G.; Krstić, S.; Pantelić, D.; Dulić, T. Cyanobacterial blooms and their
997 toxicity in Vojvodina Lakes, Serbia. *Int. J. Environ. Res.* **2013**, *7*, 745–758.
- 998 83. Paerl, H.W.W.; Huisman, J. Climate change: A catalyst for global expansion of harmful cyanobacterial blooms.
999 *Environ. Microbiol. Rep.* **2009**, *1*, 27–37.
- 1000 84. Zhou, B.; Shang, M.; Wang, G.; Zhang, S.; Feng, L.; Liu, X.; Wu, L.; Shan, K. Distinguishing two phenotypes of
1001 blooms using the normalised difference peak-valley index (NDPI) and Cyano-Chlorophyta index (CCI). *Sci.*
1002 *Total Environ.* **2018**, *628–629*, 848–857.
- 1003 85. Dierssen, H.M.; Kudela, R.M.; Ryan, J.P. Red and Black Tides : Quantitative Analysis of Water-Leaving Radiance
1004 and Perceived Color for Phytoplankton , Colored Dissolved Organic Matter , and Suspended Sediments Author
1005 (s) : Heidi M . Dierssen , Raphael M . Kudela , John P . Ryan and Richard C . *Limnol. Oceanogr.* **2006**, *51*, 2646–
1006 2659.
- 1007 86. Gitelson, A.; Mayo, M.; Yacobi, Y.Z.; Parparov, A.; Berman, T. The use of high-spectral-resolution radiometer
1008 data for detection of low chlorophyll concentrations in Lake Kinneret. *J. Plankton Res.* **1994**, *16*, 993–1002.
- 1009 87. Gower, J.F.R.; Brown, L.; Borstad, G.A. Observation of chlorophyll fluorescence in west coast waters of Canada
1010 using the MODIS satellite sensor. *Can. J. Remote Sens.* **2004**, *30*, 17–25.
- 1011 88. Gower, J.F.R.; Doerffer, R.; Borstad, G.A. Interpretation of the 685nm peak in water-leaving radiance spectra in
1012 terms of fluorescence, absorption and scattering, and its observation by MERIS. *Int. J. Remote Sens.* **1999**, *20*,
1013 1771–1786.
- 1014 89. Matthews, M.W.; Bernard, S.; Robertson, L. An algorithm for detecting trophic status (chlorophyll-a),
1015 cyanobacterial-dominance, surface scums and floating vegetation in inland and coastal waters. *Remote Sens.*
1016 *Environ.* **2012**, *124*, 637–652.

- 1017 90. Gitelson, A.; Garbuzov, G.; Szilagyi, F.; Mittenzwey, K.H.; Karnieli, A.; Kaiser, A. Quantitative remote sensing
1018 methods for real-time monitoring of inland waters quality. *Int. J. Remote Sens.* **1993**, *14*, 1269–1295.
- 1019 91. Le, C.; Li, Y.; Zha, Y.; Wang, Q.; Zhang, H.; Yin, B. Remote sensing of phycocyanin pigment in highly turbid
1020 inland waters in Lake Taihu, China. *Int. J. Remote Sens.* **2011**, *32*, 8253–8269.
- 1021 92. Dall’Olmo, G.; Gitelson, A.A. Effect of bio-optical parameter variability and uncertainties in reflectance
1022 measurements on the remote estimation of chlorophyll-a concentration in turbid productive waters: modeling
1023 results. *Appl. Opt.* **2006**, *45*, 3577.
- 1024 93. Lunetta, R.S.; Schaeffer, B.A.; Stumpf, R.P.; Keith, D.; Jacobs, S.A.; Murphy, M.S. Evaluation of cyanobacteria
1025 cell count detection derived from MERIS imagery across the eastern USA. *Remote Sens. Environ.* **2015**, *157*, 24–
1026 34.
- 1027 94. Oyama, Y.; Matsushita, B.; Fukushima, T. Distinguishing surface cyanobacterial blooms and aquatic
1028 macrophytes using Landsat/TM and ETM+ shortwave infrared bands. *Remote Sens. Environ.* **2015**, *157*, 35–47.
- 1029 95. Kudela, R.M.; Palacios, S.L.; Austerberry, D.C.; Accorsi, E.K.; Guild, L.S.; Torres-Perez, J. Application of
1030 hyperspectral remote sensing to cyanobacterial blooms in inland waters. *Remote Sens. Environ.* **2015**, *167*, 196–
1031 205.
- 1032 96. Medina-Cobo, M.; Domínguez, J.A.; Quesada, A.; de Hoyos, C. Estimation of cyanobacteria biovolume in water
1033 reservoirs by MERIS sensor. *Water Res.* **2014**, *63*, 10–20.
- 1034 97. Sheela, A.M.; Letha, J.; Joseph, S.; Ramachandran, K.K.; Sanalkumar, S.P. Trophic state index of a lake system
1035 using IRS (P6-LISS III) satellite imagery. *Environ. Monit. Assess.* **2011**, *177*, 575–592.
- 1036 98. Curtarelli, M.P.; Ogashawara, I.; Alcântara, E.H.; Stech, J.L. Coupling remote sensing bio-optical and three-
1037 dimensional hydrodynamic modeling to study the phytoplankton dynamics in a tropical hydroelectric
1038 reservoir. *Remote Sens. Environ.* **2015**, *157*, 185–198.
- 1039 99. Hedger, R.; Nils, O.; Malthus, T.; Atkinson, P. Coupling remote sensing with computational fluid dynamics
1040 modelling to estimate lake chlorophyll-a concentration. *Remote Sens. Environ.* **2002**, *79*, 116–122.
- 1041 100. Zhang, H.; Hu, W.; Gu, K.; Li, Q.; Zheng, D.; Zhai, S. An improved ecological model and software for short-term
1042 algal bloom forecasting. *Environ. Model. Softw.* **2013**, *48*, 152–162.
- 1043 101. Bresciani, M.; Bolpagni, R.; Laini, A.; Matta, E.; Bartoli, M.; Giardino, C. Multitemporal analysis of algal blooms
1044 with MERIS images in a deep meromictic lake. *Eur. J. Remote Sens.* **2013**, *46*, 445–458.
- 1045 102. Rügner, H.; Schwientek, M.; Beckingham, B.; Kuch, B.; Grathwohl, P. Turbidity as a proxy for total suspended
1046 solids (TSS) and particle facilitated pollutant transport in catchments. *Environ. Earth Sci.* **2013**, *69*, 373–380.
- 1047 103. Nasrabadi, T.; Ruegner, H.; Sirdari, Z.Z.; Schwientek, M.; Grathwohl, P. Using total suspended solids (TSS) and
1048 turbidity as proxies for evaluation of metal transport in river water. *Appl. Geochemistry* **2016**, *68*, 1–9.
- 1049 104. Julian, J.P.; Doyle, M.W.; Stanley, E.H. Empirical modeling of light availability in rivers. *J. Geophys. Res.*
1050 *Biogeosciences* **2008**, *113*, 1–16.
- 1051 105. Mendonça, R.; Müller, R.A.; Clow, D.; Verpoorter, C.; Raymond, P.; Tranvik, L.J.; Sobek, S. Organic carbon burial
1052 in global lakes and reservoirs. *Nat. Commun.* **2017**, *8*, 1–6.
- 1053 106. Adrian, R.; O’Reilly, C.M.; Zagarese, H.; Baines, S.B.; Hessen, D.O.; Keller, W.; Livingstone, D.M.; Sommaruga,
1054 R.; Straile, D.; Van Donk, E.; et al. Lakes as sentinels of climate change. *Limnol. Oceanogr.* **2009**, *54*, 2283–2297.
- 1055 107. Cole, J.J.; Prairie, Y.T.; Caraco, N.F.; McDowell, W.H.; Tranvik, L.J.; Striegl, R.G.; Duarte, C.M.; Kortelainen, P.;
1056 Downing, J.A.; Middelburg, J.J.; et al. Plumbing the global carbon cycle: Integrating inland waters into the
1057 terrestrial carbon budget. *Ecosystems* **2007**, *10*, 171–184.
- 1058 108. Downing, J.A.; Prairie, Y.T.; Cole, J.J.; Duarte, C.M.; Tranvik, L.J.; Striegl, R.G.; McDowell, W.H.; Kortelainen, P.;
1059 Caraco, N.F.; Melack, J.M.; et al. The global abundance and size distribution of lakes, ponds, and impoundments.
1060 *Limnol. Oceanogr.* **2006**, *51*, 2388–2397.
- 1061 109. Verpoorter, C.; Kutser, T.; Seekell, D.A.; Tranvik, L.J. A global inventory of lakes based on high-resolution
1062 satellite imagery. *Geophys. Res. Lett.* **2014**, *41*, 6396–6402.
- 1063 110. Bilotta, G.S.; Brazier, R.E. Understanding the influence of suspended solids on water quality and aquatic biota.
1064 *Water Res.* **2008**, *42*, 2849–2861.
- 1065 111. Kefford, B.J.; Zaluzniak, L.; Dunlop, J.E.; Nugegoda, D.; Choy, S.C. How are macroinvertebrates of slow flowing
1066 lotic systems directly affected by suspended and deposited sediments? *Environ. Pollut.* **2010**, *158*, 543–550.
- 1067 112. Overeem, I.; Hudson, B.D.; Syvitski, J.P.M.; Mikkelsen, A.B.; Hasholt, B.; van den Broeke, M.R.; Noël, B.P.Y.;
1068 Morlighem, M. Substantial export of suspended sediment to the global oceans from glacial erosion in Greenland.
1069 *Nat. Geosci.* **2017**, ngeo3046.

- 1070 113. Syvitski, J.P.M. Impact of Humans on the Flux of Terrestrial Sediment to the Global Coastal Ocean. *Science* (80-
1071). **2005**, *308*, 376–380.
- 1072 114. Spyarakos, E.; O'Donnell, R.; Hunter, P.D.; Miller, C.; Scott, M.; Simis, S.G.H.; Neil, C.; Barbosa, C.C.F.; Binding,
1073 C.E.; Bradt, S.; et al. Optical types of inland and coastal waters. *Limnol. Oceanogr.* **2017**.
- 1074 115. Novo, E.M.; Hansom, J.D.; Curran, P.J. The effect of sediment type on the relationship between reflectance and
1075 suspended sediment concentration. *Int. J. Remote Sens.* **1989**, *10*, 1283–1289.
- 1076 116. Shi, K.; Li, Y.; Li, L.; Lu, H. Absorption characteristics of optically complex inland waters: Implications for water
1077 optical classification. *J. Geophys. Res. Biogeosciences* **2013**, *118*, 860–874.
- 1078 117. Brando, V.E.; Braga, F.; Zaggia, L.; Giardino, C.; Bresciani, M.; Matta, E.; Bellafiore, D.; Ferrarin, C.; Maicu, F.;
1079 Benetazzo, A.; et al. High-resolution satellite turbidity and sea surface temperature observations of river plume
1080 interactions during a significant flood event. *Ocean Sci.* **2015**, *11*, 909–920.
- 1081 118. Pereira, L.S.F.F.; Andes, L.C.; Cox, A.L.; Ghulam, A. Measuring Suspended-Sediment Concentration and
1082 Turbidity in the Middle Mississippi and Lower Missouri Rivers using Landsat Data. *JAWRA J. Am. Water Resour.*
1083 *Assoc.* **2017**, *63103*, 1–11.
- 1084 119. Telmer, K.; Costa, M.; Angélica, R.S.; Araujo, E.S.; Maurice, Y. The source and fate of sediment and mercury in
1085 the Tapajos River, Para, Brazilian Amazon: Ground- and space-based evidence. *J. Environ. Manage.* **2006**, *81*, 101–
1086 113.
- 1087 120. Volpe, V.; Silvestri, S.; Marani, M. Remote sensing retrieval of suspended sediment concentration in shallow
1088 waters. *Remote Sens. Environ.* **2011**, *115*, 44–54.
- 1089 121. Sobek, S.; Tranvik, L.J.; Prairie, Y.T.; Cole, J.J. Patterns and regulation of dissolved organic carbon: An analysis
1090 of 7,500 widely distributed lakes. **2007**, *52*, 1208–1219.
- 1091 122. Tranvik, L.J.; Downing, J.A.; Cotner, J.B.; Loiselle, S.A.; Striegl, R.G.; Ballatore, T.J.; Dillon, P.; Finlay, K.; Fortino,
1092 K.; Knoll, L.B.; et al. Lakes and reservoirs as regulators of carbon cycling and climate. *Limnol. Oceanogr.* **2009**, *54*,
1093 2298–2314.
- 1094 123. Wen, Z.; Song, K.; Shang, Y.; Fang, C.; Li, L.; Lv, L.; Lv, X.; Chen, L. Carbon dioxide emissions from lakes and
1095 reservoirs of China: A regional estimate based on the calculated pCO₂. *Atmos. Environ.* **2017**, *170*, 71–81.
- 1096 124. McDonald, C.P.; Stets, E.G.; Striegl, R.G.; Butman, D. Inorganic carbon loading as a primary driver of dissolved
1097 carbon dioxide concentrations in the lakes and reservoirs of the contiguous United States. *Global Biogeochem.*
1098 *Cycles* **2013**, *27*, 285–295.
- 1099 125. Raymond, P.A.; Hartmann, J.; Lauerwald, R.; Sobek, S.; McDonald, C.; Hoover, M.; Butman, D.; Striegl, R.;
1100 Mayorga, E.; Humborg, C.; et al. Global carbon dioxide emissions from inland waters. *Nature* **2013**, *503*, 355.
- 1101 126. del Vecchio, R.; Blough, N. V Influence of Ultraviolet Radiation on the Chromophoric Dissolved Organic Matter
1102 in Natural Waters. In Proceedings of the Environmental UV Radiation: Impact on Ecosystems and Human
1103 Health and Predictive Models; Ghetti, F., Checucci, G., Bornman, J.F., Eds.; Springer Netherlands: Dordrecht,
1104 2006; pp. 203–216.
- 1105 127. Thrane, J.-E.; Hessen, D.O.; Andersen, T. The Absorption of Light in Lakes: Negative Impact of Dissolved
1106 Organic Carbon on Primary Productivity. *Ecosystems* **2014**, *17*, 1040–1052.
- 1107 128. Houser, J.N. Water color affects the stratification, surface temperature, heat content, and mean epilimnetic
1108 irradiance of small lakes. *Can. J. Fish. Aquat. Sci.* **2006**, *63*, 2447–2455.
- 1109 129. Kutser, T.; Alikas, K.; Kothawala, D.N.; Köhler, S.J. Impact of iron associated to organic matter on remote sensing
1110 estimates of lake carbon content. *Remote Sens. Environ.* **2015**, *156*, 109–116.
- 1111 130. Olmanson, L.G.; Brezonik, P.L.; Finlay, J.C.; Bauer, M.E. Comparison of Landsat 8 and Landsat 7 for regional
1112 measurements of CDOM and water clarity in lakes. *Remote Sens. Environ.* **2016**, *185*, 119–128.
- 1113 131. Bricaud, A.; Morel, A.; Prieur, L. Absorption by dissolved organic matter of the sea (yellow substance) in the
1114 UV and visible domains¹. *Limnol. Oceanogr.* **1981**, *26*, 43–53.
- 1115 132. Kutser, T.; Pierson, D.C.; Tranvik, L.; Reinart, A.; Sobek, S.; Kallio, K. Using Satellite Remote Sensing to Estimate
1116 the Colored Dissolved Organic Matter Absorption Coefficient in Lakes. *Ecosystems* **2005**, *8*, 709–720.
- 1117 133. Kutser, T.; Tranvik, L.; Pierson, D.C. Variations in colored dissolved organic matter between boreal lakes studied
1118 by satellite remote sensing. *J. Appl. Remote Sens.* **2009**, *3*, 033538.
- 1119 134. Brezonik, P.; Menken, K.D.; Bauer, M. Landsat-based remote sensing of lake water quality characteristics,
1120 including chlorophyll and colored dissolved organic matter (CDOM). *Lake Reserv. Manag.* **2005**, *21*, 373–382.
- 1121 135. Chang, N.-B.; Vannah, B. Monitoring the total organic carbon concentrations in a lake with the integrated data
1122 fusion and machine-learning (IDFM) technique. *SPIE Opt. Eng. + Appl.* **2012**, *8513*.

- 1123 136. Kutser, T.; Verpoorter, C.; Paavel, B.; Tranvik, L.J. Estimating lake carbon fractions from remote sensing data.
1124 *Remote Sens. Environ.* **2015**, *157*, 138–146.
- 1125 137. Griffin, C.G.; Finlay, J.C.; Brezonik, P.L.; Olmanson, L.; Hozalski, R.M. Limitations on using CDOM as a proxy
1126 for DOC in temperate lakes. *Water Res.* **2018**, *144*, 719–727.
- 1127 138. Griffin, C.G.; Frey, K.E.; Rogan, J.; Holmes, R.M. Spatial and interannual variability of dissolved organic matter
1128 in the Kolyma River, East Siberia, observed using satellite imagery. *J. Geophys. Res. Biogeosciences* **2011**, *116*, 1–
1129 12.
- 1130 139. G. Coble, P. Marine Optical Biogeochemistry: The Chemistry of Ocean Color. *Chem. Rev.* **2007**, *107*, 402–418.
- 1131 140. Cialdi, A.; Secchi, P.A. Sur la transparence de la mer. *Comptes rendus Hebd. seances l'Academie des Sci.* **1865**, *61*,
1132 100–104.
- 1133 141. Wernand, M.R. On the history of the Secchi disc. *J. Eur. Opt. Soc.* **2010**, *5*.
- 1134 142. Mazumder, A.; Taylor, W.D. Thermal Structure of Lakes Varying in Size and Water Clarity. *Limnol. Oceanogr.*
1135 **1994**, *39*, 968–976.
- 1136 143. Gunn, J.M.; Snucins, E.D.E.D.; Yan, N.D.; Arts, M.T. Use of water clarity to monitor the effects of climate change
1137 and other stressors on oligotrophic lakes. *Environ. Monit. Assess.* **2001**, *67*, 69–88.
- 1138 144. Heiskanen, J.J.; Mammarella, L.; Ojala, A.; Stepanenko, V.; Erkkilä, K.M.; Miettinen, H.; Sandström, H.; Eugster,
1139 W.; Leppäranta, M.; Järvinen, H.; et al. Effects of water clarity on lake stratification and lake-atmosphere heat
1140 exchange. *J. Geophys. Res.* **2015**, *120*, 7412–7428.
- 1141 145. Obrador, B.; Staehr, P.A.; Christensen, J.P.C. Vertical patterns of metabolism in three contrasting stratified lakes.
1142 *Limnol. Oceanogr.* **2014**, *59*, 1228–1240.
- 1143 146. Schwarz, A.M.; Hawes, I. Effects of changing water clarity on characean biomass and species composition in a
1144 large oligotrophic lake. *Aquat. Bot.* **1997**, *56*, 169–181.
- 1145 147. Izagirre, O.; Serra, A.; Guasch, H.; Elosegi, A. Effects of sediment deposition on periphytic biomass,
1146 photosynthetic activity and algal community structure. *Sci. Total Environ.* **2009**, *407*, 5694–5700.
- 1147 148. Rose, K.C.; Greb, S.R.; Diebel, M.; Turner, M.G. Annual precipitation regulates spatial and temporal drivers of
1148 lake water clarity. *Ecol. Appl.* **2017**, *27*, 632–643.
- 1149 149. Nelson, S.A.C.; Soranno, P.A.; Cheruvilil, K.S.; Batzli, S.A.; Skole, D.L. Regional Assessment of lake water clarity
1150 using satellite remote sensing. *J. Limnol.* **2003**, *62*, 27–32.
- 1151 150. Hicks, B.J.; Stichbury, G.A.; Brabyn, L.K.; Allan, M.G.; Ashraf, S. Hindcasting water clarity from Landsat satellite
1152 images of unmonitored shallow lakes in the Waikato region, New Zealand. *Environ. Monit. Assess.* **2013**, *185*,
1153 7245–7261.
- 1154 151. Bayley, S.E.; Creed, I.F.; Sass, G.Z.; Wong, A.S. Frequent regime shifts in trophic states in shallow lakes on the
1155 Boreal Plain: Alternative “unstable” states? *Limnol. Oceanogr.* **2007**, *52*, 2002–2012.
- 1156 152. Wu, G.; De Leeuw, J.; Skidmore, A.K.; Prins, H.H.T.; Liu, Y. Comparison of MODIS and Landsat TM5 images
1157 for mapping tempo–spatial dynamics of Secchi disk depths in Poyang Lake National Nature Reserve, China.
1158 *Int. J. Remote Sens.* **2008**, *29*, 2183–2198.
- 1159 153. Verdin, J.P. Bureau of Reclamation Monitoring Water Quality Conditions in a Large Western Reservoir with
1160 Landsat Imagery. *Photogramm. Eng. Remote Sensing* **1985**, *51*, 343–353.
- 1161 154. Hutchinson, E. Marginalia: Eutrophication: The scientific background of a contemporary practical problem on
1162 JSTOR. *Sigma Xi, Sci. Res. Soc.* **1973**, *61*, 269–279.
- 1163 155. Carlson, R.E. A trophic state index for lakes. *Limnol. Oceanogr.* **1977**, *22*, 361–369.
- 1164 156. Megard, R.O.; Settles, J.C.; Boyer, H.A.; Combs, W.S. Light, Secchi Disks, and Trophic States. *Limnol. Oceanogr.*
1165 **1980**, *25*, 373–377.
- 1166 157. Olmanson, L.G.; Bauer, M.E.; Brezonik, P.L. A 20-year Landsat water clarity census of Minnesota’s 10,000 lakes.
1167 *Remote Sens. Environ.* **2008**, *112*, 4086–4097.
- 1168 158. Peckham, S.D.; Chipman, J.W.; Lillesand, T.M.; Dodson, S.I. Alternate stable states and the shape of the lake
1169 trophic distribution. *Hydrobiologia* **2006**, *571*, 401–407.
- 1170 159. Politi, E.; Cutler, M.E.J.; Rowan, J.S. Evaluating the spatial transferability and temporal repeatability of remote-
1171 sensing-based lake water quality retrieval algorithms at the European scale: a meta-analysis approach. *Int. J.*
1172 *Remote Sens.* **2015**, *36*, 2995–3023.
- 1173 160. Carpenter, D.J.; Carpenter, S.M. Modeling inland water quality using Landsat data. *Remote Sens. Environ.* **1983**,
1174 *13*, 345–352.
- 1175 161. Mishra, S.; Mishra, D.R. Normalized difference chlorophyll index: A novel model for remote estimation of

- 1176 chlorophyll-a concentration in turbid productive waters. *Remote Sens. Environ.* **2012**, *117*, 394–406.
- 1177 162. Gower, J.; King, S.; Borstad, G.; Brown, L. Detection of intense plankton blooms using the 709 nm band of the
1178 MERIS imaging spectrometer. *Int. J. Remote Sens.* **2005**, *26*, 2005–2012.
- 1179 163. Hu, C. A novel ocean color index to detect floating algae in the global oceans. *Remote Sens. Environ.* **2009**, *113*,
1180 2118–2129.
- 1181 164. Shahzad, M.I.; Meraj, M.; Nazeer, M.; Zia, I.; Inam, A.; Mehmood, K.; Zafar, H. Empirical estimation of
1182 suspended solids concentration in the Indus Delta Region using Landsat-7 ETM+ imagery. *J. Environ. Manage.*
1183 **2018**, *209*, 254–261.
- 1184 165. Huang, C.; Li, Y.; Yang, H.; Sun, D.; Yu, Z.; Zhang, Z.; Chen, X.; Xu, L. Detection of algal bloom and factors
1185 influencing its formation in Taihu Lake from 2000 to 2011 by MODIS. *Environ. Earth Sci.* **2014**, *71*, 3705–3714.
- 1186 166. Morel, A. BIO-OPTICAL MODELS. **2001**, 385–394.
- 1187 167. Morel Prieur, L., A. Analysis of variations in ocean color. *Limnol. Ocean.* **1977**, *22*, 709–725.
- 1188 168. Philpot, W.D. Radiative transfer in stratified waters: a single-scattering approximation for irradiance. *Appl. Opt.*
1189 **1987**, *26*, 4123.
- 1190 169. Gordon, H.R.; Brown, O.B.; Evans, R.H.; Brown, J.W.; Smith, R.C.; Baker, K.S.; Clark, D.K. A semianalytic
1191 radiance model of ocean color. *J. Geophys. Res.* **1988**, *93*, 10909.
- 1192 170. Gordon, H.R.; Brown, O.B.; Jacobs, M.M. Computed Relationships Between the Inherent and Apparent Optical
1193 Properties of a Flat Homogeneous Ocean. *Appl. Opt.* **1975**, *14*, 417.
- 1194 171. Mobley, C.D.; Sundman, L.K. HydroLight 5 EcoLight 5 Technical documentation. *Sequoia Sci. Inc.* 2008.
- 1195 172. Dekker, A.G.; Seyhan, E.; Malthus, T.J. Quantitative Modeling of Inland Water Quality for High-Resolution MSS
1196 Systems. *IEEE Trans. Geosci. Remote Sens.* **1991**, *29*, 89–95.
- 1197 173. Kutser, T.; Arst, H. Remote sensing reflectance model of optically active components of turbid waters. In
1198 Proceedings of the Proc. SPIE 2319, Oceanic Remote Sensing and Sea Ice Monitoring; 1994; Vol. 2319, pp. 85–91.
- 1199 174. Heege, T.; Kiselev, V.; Wettle, M.; Hung, N.N. Operational multi-sensor monitoring of turbidity for the entire
1200 Mekong Delta. *Int. J. Remote Sens.* **2014**, *35*, 2910–2926.
- 1201 175. Lymburner, L.; Botha, E.; Hestir, E.; Anstee, J.; Sagar, S.; Dekker, A.; Malthus, T. Landsat 8: Providing continuity
1202 and increased precision for measuring multi-decadal time series of total suspended matter. *Remote Sens. Environ.*
1203 **2016**, *185*, 108–118.
- 1204 176. Zhou, X.; Marani, M.; Albertson, J.; Silvestri, S.; Zhou, X.; Marani, M.; Albertson, J.D.; Silvestri, S. Hyperspectral
1205 and Multispectral Retrieval of Suspended Sediment in Shallow Coastal Waters Using Semi-Analytical and
1206 Empirical Methods. *Remote Sens.* **2017**, *9*, 393.
- 1207 177. Dekker, A.G.; Vos, R.J.; Peters, S.W.M. Analytical algorithms for lake water TSM estimation for retrospective
1208 analyses of TM and SPOT sensor data. *Int. J. Remote Sens.* **2002**, *23*, 15–35.
- 1209 178. Dekker, A.G.; Vos, R.J.; Peters, S.W.M. Comparison of remote sensing data, model results and in situ data for
1210 total suspended matter (TSM) in the southern Frisian lakes. *Sci. Total Environ.* **2001**, *268*, 197–214.
- 1211 179. Olden, J.D.; Lawler, J.J.; Poff, N.L. Machine Learning Methods Without Tears: A Primer for Ecologists. *Q. Rev.*
1212 *Biol.* **2008**, *83*, 171–193.
- 1213 180. Camps-Valls, G. Machine learning in remote sensing data processing. In Proceedings of the 2009 IEEE
1214 International Workshop on Machine Learning for Signal Processing; IEEE, 2009; pp. 1–6.
- 1215 181. Lary, D.J.; Alavi, A.H.; Gandomi, A.H.; Walker, A.L. Machine learning in geosciences and remote sensing.
1216 *Geosci. Front.* **2016**, *7*, 3–10.
- 1217 182. Imen, S.; Chang, N. Bin; Yang, Y.J. Developing the remote sensing-based early warning system for monitoring
1218 TSS concentrations in Lake Mead. *J. Environ. Manage.* **2015**, *160*, 73–89.
- 1219 183. Song, K. Water quality monitoring using Landsat Themate Mapper data with empirical algorithms in Chagan
1220 Lake, China. *J. Appl. Remote Sens.* **2011**, *5*, 053506.
- 1221 184. Schiller, H.; Doerffer, R. Neural network for emulation of an inverse model operational derivation of Case II
1222 water properties from MERIS data. *Int. J. Remote Sens.* **1999**, *20*, 1735–1746.
- 1223 185. Song, K.; Li, L.; Tedesco, L.P.; Li, S.; Duan, H.; Liu, D.; Hall, B.E.; Du, J.; Li, Z.; Shi, K.; et al. Remote estimation
1224 of chlorophyll-a in turbid inland waters: Three-band model versus GA-PLS model. *Remote Sens. Environ.* **2013**,
1225 *136*, 342–357.
- 1226 186. Chang, N.-B.; Vannah, B.W.; Yang, Y.J.; Elovitz, M. Integrated data fusion and mining techniques for monitoring
1227 total organic carbon concentrations in a lake. *Int. J. Remote Sens.* **2014**, *35*, 1064–1093.
- 1228 187. Sun, D.; Qiu, Z.; Li, Y.; Shi, K.; Gong, S. Detection of Total Phosphorus Concentrations of Turbid Inland Waters

- 1229 Using a Remote Sensing Method. *Water, Air, Soil Pollut.* **2014**, *225*, 1953.
- 1230 188. Lin, S.; Novitski, L.N.; Qi, J.; Stevenson, R.J. Landsat TM/ETM+ and machine-learning algorithms for
1231 limnological studies and algal bloom management of inland lakes. *J. Appl. Remote Sens.* **2018**, *12*, 1–17.
- 1232 189. Qi, L.; Hu, C.; Duan, H.; Barnes, B.B.; Ma, R. An EOF-based algorithm to estimate chlorophyll a concentrations
1233 in taihu lake from MODIS land-band measurements: Implications for near real-time applications and forecasting
1234 models. *Remote Sens.* **2014**, *6*, 10694–10715.
- 1235 190. Duan, H.; Tao, M.; Loisel, S.A.; Zhao, W.; Cao, Z.; Ma, R.; Tang, X. MODIS observations of cyanobacterial risks
1236 in a eutrophic lake: Implications for long-term safety evaluation in drinking-water source. *Water Res.* **2017**, *122*,
1237 455–470.
- 1238 191. Hastie, T.T. The Elements of Statistical Learning. *Math. Intell.* **2009**, *27*, 83–85.
- 1239 192. Rocha, A.D.; Groen, T.A.; Skidmore, A.K.; Darvishzadeh, R.; Willems, L. The Naïve Overfitting Index Selection
1240 (NOIS): A new method to optimize model complexity for hyperspectral data. *ISPRS J. Photogramm. Remote Sens.*
1241 **2017**, *133*, 61–74.
- 1242 193. Xiang, B.; Song, J.-W.; Wang, X.-Y.; Zhen, J. Improving the accuracy of estimation of eutrophication state index
1243 using a remote sensing data-driven method: A case study of Chaohu Lake, China. *Water SA* **2015**, *41*, 753.
- 1244 194. Concha, J.A.; Schott, J.R. Retrieval of color producing agents in Case 2 waters using Landsat 8. *Remote Sens.*
1245 *Environ.* **2016**, *185*, 95–107.
- 1246 195. Pahlevan, N.; Sarkar, S.; Franz, B.A.; Balasubramanian, S. V.; He, J. Sentinel-2 MultiSpectral Instrument (MSI)
1247 data processing for aquatic science applications: Demonstrations and validations. *Remote Sens. Environ.* **2017**,
1248 *201*, 47–56.
- 1249 196. Brivio, P.A.; Giardino, C.; Zilioli, E. Validation of satellite data for quality assurance in lake monitoring
1250 applications. *Sci. Total Environ.* **2001**, *268*, 3–18.
- 1251 197. Gordon, H.R.; Wang, M. Retrieval of water-leaving radiance and aerosol optical thickness over the oceans with
1252 SeaWiFS: a preliminary algorithm. *Appl. Opt.* **1994**, *33*, 443.
- 1253 198. Schroeder, T.; Behnert, I.; Schaale, M.; Fischer, J.; Doerffer, R. Atmospheric correction algorithm for MERIS above
1254 case-2 waters. *Int. J. Remote Sens.* **2007**, *28*, 1469–1486.
- 1255 199. Vanhellemont, Q.; Ruddick, K. Atmospheric correction of metre-scale optical satellite data for inland and coastal
1256 water applications. *Remote Sens. Environ.* **2018**, *216*, 586–597.
- 1257 200. Wang, M.; Son, S.; Zhang, Y.; Shi, W. Remote sensing of water optical property for China’s inland lake taihu
1258 using the SWIR atmospheric correction with 1640 and 2130 nm bands. *IEEE J. Sel. Top. Appl. Earth Obs. Remote*
1259 *Sens.* **2013**, *6*, 2505–2516.
- 1260 201. Novoa, S.; Doxaran, D.; Ody, A.; Vanhellemont, Q.; Lafon, V.; Lubac, B.; Gernez, P. Atmospheric corrections and
1261 multi-conditional algorithm for multi-sensor remote sensing of suspended particulate matter in low-to-high
1262 turbidity levels coastal waters. *Remote Sens.* **2017**, *9*.
- 1263 202. Pahlevan, N.; Chittimalli, S.K.; Balasubramanian, S. V.; Vellucci, V. Sentinel-2/Landsat-8 product consistency
1264 and implications for monitoring aquatic systems. *Remote Sens. Environ.* **2019**, *220*, 19–29.
- 1265 203. Kiselev, V.; Bulgarelli, B.; Heege, T. Sensor independent adjacency correction algorithm for coastal and inland
1266 water systems. *Remote Sens. Environ.* **2015**, *157*, 85–95.
- 1267 204. Garaba, S.P.; Zielinski, O. An assessment of water quality monitoring tools in an estuarine system. *Remote Sens.*
1268 *Appl. Soc. Environ.* **2015**, *2*, 1–10.
- 1269 205. Garaba, S.; Badewien, T.H.; Braun, A.; Schulz, A.C.; Zielinski, O. Using ocean colour remote sensing products
1270 to estimate turbidity at the Wadden sea time series station Spiekeroog. *J. Eur. Opt. Soc.* **2014**, *9*.
- 1271 206. Kutser, T.; Vahtmäe, E.; Praks, J. A sun glint correction method for hyperspectral imagery containing areas with
1272 non-negligible water leaving NIR signal. *Remote Sens. Environ.* **2009**, *113*, 2267–2274.
- 1273 207. Martin, J.; Eugenio, F.; Marcello, J.; Medina, A. Automatic sun glint removal of multispectral high-resolution
1274 WorldView-2 imagery for retrieving coastal shallow water parameters. *Remote Sens.* **2016**, *8*, 1–16.
- 1275 208. Doxaran, D.; Froidefond, J.M.; Castaing, P. A reflectance band ratio used to estimate suspended matter
1276 concentrations in sediment-dominated coastal waters A re ectance band ratio used to estimate suspended matter
1277 concentrations in sediment-dominated coastal w. *Int. J. Remote Sens.* **2002**, *23*, 5079–5085.
- 1278 209. Bukata, R.P. Retrospection and introspection on remote sensing of inland water quality : “ Like Déjà Vu All Over
1279 Again .” *J. Great Lakes Res.* **2013**, *39*, 2–5.
- 1280 210. Downing, J.A. Limnology and oceanography: Two estranged twins reuniting by global change. *Inl. Waters* **2014**,
1281 *4*, 215–232.

- 1282 211. Palmer, S.C.J.; Kutser, T.; Hunter, P.D. Remote sensing of inland waters: Challenges, progress and future
1283 directions. *Remote Sens. Environ.* **2015**, *157*, 1–8.
- 1284 212. Aria, M.; Cuccurullo, C. bibliometrix: An R-tool for comprehensive science mapping analysis. *J. Informetr.* **2017**,
1285 *11*, 959–975.
- 1286 213. Bornmann, L.; Mutz, R. Growth rates of modern science: A bibliometric analysis based on the number of
1287 publications and cited references. *J. Assoc. Inf. Sci. Technol.* **2015**, *66*, 2215–2222.
- 1288 214. Wulder, M.A.; Masek, J.G.; Cohen, W.B.; Loveland, T.R.; Woodcock, C.E. Opening the archive: How free data
1289 has enabled the science and monitoring promise of Landsat. *Remote Sens. Environ.* **2012**, *122*, 2–10.
- 1290 215. Willmott, C.J. On the validation of Models. *Phys. Geogr.* **1981**, *2*, 184–194.
- 1291 216. Alikas, K.; Reinart, A. Validation of the MERIS products on large European lakes: Peipsi, Vänern and Vättern.
1292 *Hydrobiologia* **2008**, *599*, 161–168.
- 1293 217. Kallio, K.; Koponen, S.; Ylöstalo, P.; Kervinen, M.; Pyhälähti, T.; Attila, J. Validation of MERIS spectral inversion
1294 processors using reflectance, IOP and water quality measurements in boreal lakes. *Remote Sens. Environ.* **2015**,
1295 *157*, 147–157.
- 1296 218. Okullo, W.; Hamre, B.; Frette, O.; Stamnes, J.J.; Sorensen, K.; Ssenyonga, T.; Hokedal, J.; Stamnes, K.; Steigen, A.
1297 Validation of MERIS water quality products in Murchison Bay, Lake Victoria - Preliminary results. *Int. J. Remote*
1298 *Sens.* **2011**, *32*, 5541–5563.
- 1299 219. Therneau, T.; Atkinson, B. rpart: Recursive Partitioning and Regression Trees. 2019.
- 1300 220. Venables, W.N.; Ripley, B.D. *Modern Applied Statistics with S*; Fourth.; Springer: New York, 2002; ISBN 0-387-
1301 95457-0.
- 1302 221. Pedregosa, F.; Varoquaux, G.; Gramfort, A.; Michel, V.; Thirion, B.; Grisel, O.; Blondel, M.; Müller, A.; Nothman,
1303 J.; Louppe, G.; et al. Scikit-learn: Machine Learning in Python. **2011**, *12*, 2825–2830.
- 1304 222. Sonnenburg, S.; Braun, M.; Ong, C.S.; Bengio, S.; Botou, L.; Holmes, G.; LeCun, Y.; Muller, K.-R.; Pereira, F.;
1305 Rasmussen, C.E.; et al. The Need for Open Source Software in Machine Learning. *J. Mach. Learn. Res.* **2007**, *8*,
1306 600–611.
- 1307 223. Pearson, K. Mathematical contributions to the theory of evolution. III. Regression, heredity, and panmixia.
1308 *Philos. Trans. R. Soc. London. Ser. A, Contain. Pap. a Math. or Phys. character* **1896**, *187*, 253–318.
- 1309 224. Olmanson, L.G.; Brezonik, P.L.; Bauer, M.E. Geospatial and temporal analysis of a 20-year record of Landsat-
1310 based water clarity in Minnesota’s 10,000 lakes. *J. Am. Water Resour. Assoc.* **2014**, *50*, 748–761.
- 1311 225. Ng, S.M.Y.; Antenucci, J.P.; Hipsey, M.R.; Tibor, G.; Zohary, T. Physical controls on the spatial evolution of a
1312 dinoflagellate bloom in a large lake. *Limnol. Oceanogr.* **2011**, *56*, 2265–2281.
- 1313 226. Wang, M.; Nim, C.J.; Son, S.H.; Shi, W. Characterization of turbidity in Florida’s Lake Okeechobee and
1314 Caloosahatchee and St. Lucie Estuaries using MODIS-Aqua measurements. *Water Res.* **2012**, *46*, 5410–5422.
- 1315 227. Zhu, M.; Paerl, H.W.; Zhu, G.; Wu, T.; Li, W.; Shi, K.; Zhao, L.; Zhang, Y.; Qin, B.; Caruso, A.M. The role of
1316 tropical cyclones in stimulating cyanobacterial (*Microcystis* spp.) blooms in hypertrophic Lake Taihu, China.
1317 *Harmful Algae* **2014**, *39*, 310–321.
- 1318 228. Sass, G.Z.; Creed, I.F.; Bayley, S.E.; Devito, K.J. Interannual variability in trophic status of shallow lakes on the
1319 Boreal Plain: Is there a climate signal? *Water Resour. Res.* **2008**, *44*, 1–11.
- 1320 229. Cui, L.; Qiu, Y.; Fei, T.; Liu, Y.; Wu, G. Using remotely sensed suspended sediment concentration variation to
1321 improve management of Poyang Lake, China. *Lake Reserv. Manag.* **2013**, *29*, 47–60.
- 1322 230. Cui, L.; Wu, G.; Liu, Y. Monitoring the impact of backflow and dredging on water clarity using MODIS images
1323 of Poyang Lake, China. *Hydrol. Process.* **2009**, *23*, 342–350.
- 1324 231. Ren, J.; Zheng, Z.; Li, Y.; Lv, G.; Wang, Q.; Lyu, H.; Huang, C.; Liu, G.; Du, C.; Mu, M.; et al. Remote observation
1325 of water clarity patterns in Three Gorges Reservoir and Dongting Lake of China and their probable linkage to
1326 the Three Gorges Dam based on Landsat 8 imagery. *Sci. Total Environ.* **2018**, *625*, 1554–1566.
- 1327 232. Hou, X.; Feng, L.; Duan, H.; Chen, X.; Sun, D.; Shi, K. Fifteen-year monitoring of the turbidity dynamics in large
1328 lakes and reservoirs in the middle and lower basin of the Yangtze River, China. *Remote Sens. Environ.* **2017**, *190*,
1329 107–121.
- 1330 233. Pavelsky, T.M.; Smith, L.C. Remote sensing of suspended sediment concentration, flow velocity, and lake
1331 recharge in the Peace-Athabasca Delta, Canada. *Water Resour. Res.* **2009**, *45*, 1–16.
- 1332 234. Long, C.M.; Pavelsky, T.M. Remote sensing of suspended sediment concentration and hydrologic connectivity
1333 in a complex wetland environment. *Remote Sens. Environ.* **2013**, *129*, 197–209.
- 1334 235. Sandström, A.; Philipson, P.; Asp, A.; Axenrot, T.; Kinnerbäck, A.; Ragnarsson-Stabo, H.; Holmgren, K.

- 1335 Assessing the potential of remote sensing-derived water quality data to explain variations in fish assemblages
 1336 and to support fish status assessments in large lakes. *Hydrobiologia* **2016**, *780*, 71–84.
- 1337 236. Torbick, N.; Hession, S.; Stommel, E.; Caller, T. Mapping amyotrophic lateral sclerosis lake risk factors across
 1338 northern New England. *Int. J. Health Geogr.* **2014**, *13*.
- 1339 237. Finger, F.; Knox, A.; Bertuzzo, E.; Mari, L.; Bompangue, D.; Gatto, M.; Rodriguez-Iturbe, I.; Rinaldo, A. Cholera
 1340 in the Lake Kivu region (DRC): Integrating remote sensing and spatially explicit epidemiological modeling.
 1341 *Water Resour. Res.* **2014**, *50*, 5624–5637.
- 1342 238. McCullough, I.M.; Loftin, C.S.; Sader, S.A. Landsat imagery reveals declining clarity of Maine’s lakes during
 1343 1995–2010. *Freshw. Sci.* **2013**, *32*, 741–752.
- 1344 239. Gorelick, N.; Hancher, M.; Dixon, M.; Ilyushchenko, S.; Thau, D.; Moore, R. Google Earth Engine: Planetary-
 1345 scale geospatial analysis for everyone. *Remote Sens. Environ.* **2017**, *202*, 18–27.
- 1346 240. Fox, J. Aspects of the Social Organization and Trajectory of the R Project. *R J.* **2009**, *1*.
- 1347 241. Read, E.K.; Carr, L.; De Cicco, L.; Dugan, H.A.; Hanson, P.C.; Hart, J.A.; Kreft, J.; Read, J.S.; Winslow, L.A. Water
 1348 quality data for national-scale aquatic research: The Water Quality Portal. *Water Resour. Res.* **2017**, *53*, 1735–1745.
- 1349 242. Soranno, P.A.; Bacon, L.C.; Beauchene, M.; Bednar, K.E.; Bissell, E.G.; Boudreau, C.K.; Boyer, M.G.; Bremigan,
 1350 M.T.; Carpenter, S.R.; Carr, J.W.; et al. LAGOS-NE: A multi-scaled geospatial and temporal database of lake
 1351 ecological context and water quality for thousands of U.S. lakes. *Gigascience* **2017**, 1–22.
- 1352 243. Schaeffer, B.A.; Iames, J.; Dwyer, J.; Urquhart, E.; Salls, W.; Rover, J.; Seegers, B. An initial validation of Landsat
 1353 5 and 7 derived surface water temperature for U.S. lakes, reservoirs, and estuaries. *Int. J. Remote Sens.* **2018**, *00*,
 1354 1–17.
- 1355 244. Srebotnjak, T.; Carr, G.; De Sherbinin, A.; Rickwood, C. A global Water Quality Index and hot-deck imputation
 1356 of missing data. *Ecol. Indic.* **2012**, *17*, 108–119.
- 1357 245. Ross, M.R.V.; Topp, S.N.; Appling, A.; Yang, X.; Kuhn, C.; Buttman, D.; Simard, M.; Pavelsky, T. AquaSat: a
 1358 dataset to enable remote sensing of water quality for inland waters. *Water Resour. Res.*
- 1359 246. Kneubühler, M.; Damm-Reiser, A. Recent progress and developments in imaging spectroscopy. *Remote Sens.*
 1360 **2018**, *10*, 1–4.
- 1361 247. Cooley, S.W.; Smith, L.C.; Stepan, L.; Mascaro, J. Tracking dynamic northern surface water changes with high-
 1362 frequency planet CubeSat imagery. *Remote Sens.* **2017**, *9*, 1–21.
- 1363 248. McCabe, M.F.; Rodell, M.; Alsdorf, D.E.; Miralles, D.G.; Uijlenhoet, R.; Wagner, W.; Lucieer, A.; Houborg, R.;
 1364 Verhoest, N.E.C.; Franz, T.E.; et al. The future of Earth observation in hydrology. *Hydrol. Earth Syst. Sci.* **2017**,
 1365 *21*, 1–56.
- 1366 249. Devred, E.; Turpie, K.R.; Moses, W.; Klemas, V. V.; Moisan, T.; Babin, M.; Toro-Farmer, G.; Forget, M.H.; Jo, Y.H.
 1367 Future retrievals of water column bio-optical properties using the hyperspectral infrared imager (hyspirci).
 1368 *Remote Sens.* **2013**, *5*, 6812–6837.
- 1369 250. IOCCG. Why Ocean Colour? The Societal Benefits of Ocean-Colour Technology. Platt, T., Hoepffner, N., Stuart,
 1370 V. and Brown, C. (eds.), Reports of the International Ocean-Colour Coordinating Group, No. 7, **2008**;
- 1371 251. National Academies of Sciences, E. and M. *Thriving on Our Changing Planet*; National Academies Press:
 1372 Washington, D.C., **2018**; ISBN 978-0-309-46757-5.
- 1373 252. Poikane, S.; Van Den Berg, M.; Hellsten, S.; De Hoyos, C.; Ortiz-Casas, J.; Pall, K.; Portielje, R.; Phillips, G.;
 1374 Solheim, A.L.; Tierney, D.; et al. Lake ecological assessment systems and intercalibration for the European Water
 1375 Framework Directive: Aims, achievements and further challenges. *Procedia Environ. Sci.* **2011**, *9*, 153–168.
- 1376 253. Wu, G.; de Leeuw, J.; Skidmore, A.K.; Prins, H.H.T.T.; Liu, Y. Concurrent monitoring of vessels and water
 1377 turbidity enhances the strength of evidence in remotely sensed dredging impact assessment. *Water Res.* **2007**,
 1378 *41*, 3271–3280.
- 1379 254. Robert, E.; Kergoat, L.; Soumaguel, N.; Merlet, S.; Martinez, J.M.; Diawara, M.; Grippa, M. Analysis of suspended
 1380 particulate matter and its drivers in Sahelian Ponds and Lakes by remote sensing (landsat and MODIS): Gourma
 1381 Region, Mali. *Remote Sens.* **2017**, *9*.
- 1382 255. Huang, C.; Guo, Y.; Yang, H.; Li, Y.; Zou, J.; Zhang, M.; Lyu, H.; Zhu, A.; Huang, T. Using Remote Sensing to
 1383 Track Variation in Phosphorus and Its Interaction with Chlorophyll-a and Suspended Sediment. *IEEE J. Sel. Top.*
 1384 *Appl. Earth Obs. Remote Sens.* **2015**, *8*, 4171–4180.
- 1385 256. Duane Nellis, M.; Harrington, J. a.; Wu, J. Remote sensing of temporal and spatial variations in pool size,
 1386 suspended sediment, turbidity, and Secchi depth in Tuttle Creek Reservoir, Kansas: 1993. *Geomorphology* **1998**,
 1387 *21*, 281–293.

- 1388 257. Feng, L.; Hu, C.; Han, X.; Chen, X.; Qi, L. Long-term distribution patterns of chlorophyll-a concentration in
 1389 China's largest freshwater lake: MERIS full-resolution observations with a practical approach. *Remote Sens.* **2015**,
 1390 *7*, 275–299.
- 1391 258. Sass, G.Z.; Creed, I.F.; Devito, K.J. Spatial heterogeneity in trophic status of shallow lakes on the Boreal Plain:
 1392 Influence of hydrologic setting. *Water Resour. Res.* **2008**, *44*.
- 1393 259. Potes, M.; Costa, M.J.; Salgado, R. Satellite remote sensing of water turbidity in Alqueva reservoir and
 1394 implications on lake modelling. *Hydrol. Earth Syst. Sci.* **2012**, *16*, 1623–1633.
- 1395

1396 **Author Contributions:** Conceptualization and methodology conducted by S.T., M.R., and T.P. Formal analysis done
 1397 by S.T, M.R., and D.J. Writing and draft preparation done by S.T. Review and editing done by S.T., M.R., T.P., D.J., and
 1398 M.S. All authors contributed substantially to the produced work.

1399 **Funding:** Support for the manuscript was provided by NASA NESSF 80NSSC18K1398. Part of this work was
 1400 conducted at the Jet Propulsion Laboratory, California Institute of Technology, under a contract with the National
 1401 Aeronautics and Space Administration.

1402 **Acknowledgments** We are grateful to all those who provided feedback on this manuscript.

1403 **Appendix A: Supplemental Information**

1404 The inland water quality remote sensing index can be found in its entirety here:

1405 [https://docs.google.com/spreadsheets/d/1GMka4B-E16FmXBWjv0lhBN0T-](https://docs.google.com/spreadsheets/d/1GMka4B-E16FmXBWjv0lhBN0T-07oeZT4riepMMHvZz4/edit?usp=sharingusp=sharing)
 1406 [07oeZT4riepMMHvZz4/edit?usp=sharingusp=sharing](https://docs.google.com/spreadsheets/d/1GMka4B-E16FmXBWjv0lhBN0T-07oeZT4riepMMHvZz4/edit?usp=sharingusp=sharing)

1407 The code and data for all analysis and figures can be found here:

1408 <https://github.com/SimonTopp/rs.iw.review>

1409 The supplemental tables below describe in detail the recorded metrics of each included study as well
 1410 as a description of the studies identified as applying remote sensing to better understand the dynamics and
 1411 impacts of inland water quality.

1412

Index Parameter	Parameter Description
Identifying information	Composed of an index number, author(s), journal, title, year of publication, DOI, and total citation count pulled from SCOPUS.
Locational Information	Country of focus and central latitude and longitude of the study area.
Study Scale	The order of magnitude of the study area in km ² . The surface area of the waterbody for single waterbody studies, total area of all waterbodies for spatially discontinuous studies, or the total area of the entire region if the study area was contiguous. Represented as 10 ¹ km ² , 10 ² km ² , 10 ³ km ² , etc.
Study Period	The duration of the study. If no temporal analysis was conducted than the period was marked na. Total study length was determined as the date of the first image to the date of the final image.
Sensor Information	Satellite and/or airborne sensors utilized and the spectral resolution of each sensor (hyperspectral or multispectral)
Atmospheric Correction	A binary yes/no regarding the application of an atmospheric correction for the final model.
Parameters	The water quality parameters included in the study.
Waterbody Type	The waterbody of focus (Rivers, Lakes/Reservoirs, Estuaries, or Deltas)
Modeling Approach Information	The model inputs, chosen modelling methodology, and total number of models used. Also included is information on if different modelling approaches were compared (i.e. empirical vs semi-analytical approaches).
Number of Methodology Figures	The total count of figures focused on background information. These include study area maps, flow charts, tables with input data, and other figures depicting the theory or method behind the modelling approach.
Number of Validation Figures	The total count of figures focused on model validation. These include tables of error metrics and actual vs. predicted plots.
Number of Trend, Impact, and Driver Figures	The total count of figures and tables depicting some spatial or temporal trend. These include maps, timelines, figures depicting correlations between water quality parameters and climatic or anthropogenic drivers, and figures or tables examining the impacts of changing water quality parameters on ecological or anthropogenic systems.
Paper Category	The final classification of the paper based on total figure counts and proposed hypothesis/science questions.
Model Fit Error	Reported error metrics for model fit.
Model Validation Error	Reported error metrics for model validation based on data not used in model development.

1413

1414

Table S1. Summary of collected information for the detailed literature review index.

	Author	Scale (km ²)	Duration	Waterbody	Approach	Constituent	Analysis Summary
Anthropogenic Drivers	Ren et al., 2018	10 ³	1-5 Years	Lakes	Empirical	SDD	Examines spatiotemporal variations in water clarity and sediment discharge connected to the Three Gorges Dam. Finds that certain areas have inversely correlated clarity driven by surface flow dynamics.
	Hou et al., 2017	10 ⁵	>10 Years	Lakes	Empirical	TSS	Examines the spatiotemporal response of TSS in the Yangtze River Basin to the construction of the Three Gorges Dam. Found that the reservoir construction drove varying regional effects, and that recent improvements in TSS are likely correlated with increased NDVI in the area.
	Cui et al., 2013	10 ³	5-10 Years	Lakes	Empirical	TSS	Examines the spatiotemporal trends of TSS in a Chinese lake and how it correlates with dredging activities and climactic drivers.
	McCullough et al., 2012	10 ⁴	>10 Years	Lakes	Empirical	SDD	Utilizes Landsat data to examine water clarity in Maine over 15 years. Finds that decreased clarity is somewhat correlated to the presence of timber harvesting in a watershed.
	Cui, Wu, and Liu, 2009	10 ³	1-5 Years	Lakes	Empirical	SDD	Examines the interactions between elevated TSS levels driven by river backflow into Poyang Lake (China) and lake dredging. Finds that the combined impact is greater than either event by itself.
	Wu et al., 2007	10 ³	5-10 Years	Lakes	Empirical	SDD	Utilizes Landsat and MODIS data to measure the effect of dredging on water clarity.
Climatic Drivers	Lymburner et al., 2016	10 ⁵	>10 Years	Lakes	Semi Analytical	TSS	Examines interactions between decadal climate variations (ENSO) and TSS concentrations in optically heterogenous lakes across western Australia.
	Robert et al., 2017	10 ²	>10 Years	Lakes	Empirical	TSS	Examines climactic drivers of TSS extremes and seasonal cycles in Mali lakes.

Author	Scale (km ²)	Duration	Waterbody	Approach	Constituent	Analysis Summary
Huang et al., 2015	10 ³	< 1 Month	Lakes	Empirical	TSS, Chl-a, TP	Examines how the provision of phosphorous from sediment resuspension controls TSS and chl-a dynamics in a shallow lake.
Zhang et al., 2016	10 ³	5-10 Years	Lakes	Empirical	TSS	Analyzes spatiotemporal dynamics of river plumes in a shallow lake and their correlation with rainfall magnitude.
Zhu et al., 2014	10 ³	1-5 Years	Lakes	Semi Empirical	Algal Blooms	Examines how typhoon induced sediment resuspension and nutrient mixing impact the development dynamics of algal blooms.
Curtarelli et al., 2015	10 ²	< 1 Year	Lakes	Empirical	Chl-a	Combines remote sensing with hydrodynamic modelling to examine the role of thermal stratification and mixing on chl-a dynamics.
Matthews, 2014	10 ³	>10 Years	Lakes	Empirical	Chl-a	Identifies long term trends in chl-a and cyanobacteria blooms across 50 lakes in South Africa. Discusses how clustering of overarching trends and lake trophic state follow biogeophysical landscape properties.
Huang et al., 2014	10 ³	>10 Years	Lakes	Semi Empirical	Chl-a	Examines the role of wind, precipitation, decadal climate signals, and resuspension driven nutrient availability on the presence/dynamics of algal blooms.
Nellis, Harrington, & Wu, 1998	10 ²	< 1 Year	Lakes	Semi Analytical	TSS	Examines the impacts of a flood event on sediment concentration, pool size, and water quality dynamics in a Kansas reservoir.
Wang et al., 2012	10 ³	5-10 Years	Multiple	Empirical	Turbidity	Examines the role of hurricanes in controlling turbidity levels in Florida's Lake Okeechobee and two connected estuaries.

	Author	Scale (km ²)	Duration	Waterbody	Approach	Constituent	Analysis Summary
	Ng et al., 2011	10 ²	< 1 Year	Lakes	Semi Empirical	Chl-a	Incorporates remote sensing data into a 3D hydrological model to analyze dinoflagellate dispersion within a lake ecosystem. Finds that bloom growth is controlled by stratification while dispersion is driven by wave forces.
	Sass et al., 2008a	10 ³	>10 Years	Lakes	Empirical	Chl-a	Examines variations in trophic state within boreal lakes driven by climactic variables. Finds that growing season length and May temperatures are key drivers.
	Bayley et al., 2007	10 ²	>10 Years	Lakes	Empirical	Chl-a	Tests the 'stable states' hypothesis regarding trophic status for boreal lakes and finds that most lakes in the study area have one dominate state rather than two.
	Feng et al., 2015	10 ⁴	5-10 Years	Lakes	Semi Empirical	Chl-a	Identifies high risk eutrophication areas and their relationship to connectivity and precipitation.
	Duan et al., 2017	10 ²	>10 Years	Lakes	Machine Learning	Chl-a	Analyzes spatiotemporal distributions of phycocyanin and chl-a and develops a hazard assessment map to identify safe areas for drinking water outlets.
Landscape Level Drivers	Dvornikov et al., 2018	10 ²	Snapshot	Lakes	Empirical	CDOM	Analyzes landscape level drivers of CDOM in arctic lakes and finds significant relationships between thermocirque presence and elevated CDOM levels.
	Sass et al., 2008b	10 ³	>10 Years	Lakes	Empirical	Chl-a	Examines connectivity, wetland area, and concentrations of Ca and Mg that control the trophic state of boreal lakes.
	Rose et al., 2017	10 ⁵	>10 Years	Lakes	Empirical	SDD	Examines how watershed and riparian zone characteristics drive water clarity and finds that during wet years, watershed scale drivers dominate while for dry years riparian characteristics are more important.

	Author	Scale (km ²)	Duration	Waterbody	Approach	Constituent	Analysis Summary
Forecasting	Qin et al., 2015	10 ³	1-5 Years	Lakes	Empirical	Chl-a	Develops a dynamic forecasting model incorporating wind, precipitation, and remotely sensed chl-a concentration to predict algal bloom development in Lake Taihu, China. The applied model helped remove over 1,000,000 tons of algal scum from the lake.
	Imen et al., 2015	10 ³	1-5 Years	Lakes	Machine Learning	TSS	Utilizes remotely sensed TSS data to construct a real-time forecasting model for predicting degraded water quality near drinking water outlets in Lake Mead.
	Zhang et al., 2013	10 ³	< 1 Month	Lakes	Mixed	Chl-a	Develops forecasting model capable of predicting algal blooms 3-5 days in advance in shallow Lake Taihu in China.
Water Quality Impacts	Sandström et al., 2016	10 ³	5-10 Years	Lakes	Product	Chl-a	Utilizes remotely sensed water quality parameters to identify and explain variations in fish habitat and species composition. Found that habitat was highly correlated with CDOM and chl-a levels.
	Torbick et al., 2014	10 ⁵	1-5 Years	Lakes	Empirical	Chl-a	Examines distribution of algal blooms in relation to reported cases of amyotrophic lateral sclerosis (ALS) to identify high risk areas for the disease.
	Potes, Costa, & Salgado, 2012	10 ²	1-5 Years	Lakes	Empirical	Turbidity	Incorporates remotely sensed turbidity into a two-layer bulk model to predict surface water temperature.
	Finger et al., 2014	10 ³	5-10 Years	Lakes	Product	Chl-a	Incorporates remotely sensed chl-a data into a model examining the dynamics and drivers of cholera outbreaks in the Democratic Republic of Congo.
	Pavelsky and Smith, 2009	10 ³	< 1 Year	Lakes/River	Empirical	TSS	Utilizes remotely sensed TSS concentration to examine river velocity, flow reversal, and hydrologic recharge of floodplain lakes in the Peace-Athabasca Delta.

	Author	Scale (km ²)	Duration	Waterbody	Approach	Constituent	Analysis Summary
	Telmer et al., 2006	10 ⁵	>10 Years	Rivers	Empirical	TSS	By using the correlation between TSS and mercury, the authors present a remote estimation of mercury concentrations, which they use to examine likely drivers of increased mercury concentrations from gold-mining.
	Overeem et al., 2017	10 ⁴	>10 Years	Rivers	Empirical	TSS	Examined flux of suspended sediment from Greenland ice sheet, highlighting disproportionately high global contribution of sediment.
Water Quality Dynamics	Griffin et al., 2011	10 ⁴	5-10 Years	Rivers	Empirical	CDOM	Used remote sensing of CDOM and DOC to highlight the interannual variability of both, while also highlighting that the spatial and temporal variability likely causes underestimates of DOC flux from Kolyma River.
	Walker, 1996	10 ⁵	1-5 Years	Estuaries	Semi Analytical	TSS	With remote sensing estimates of suspended sediments, Walker explores causes of plume variability in the Mississippi River.
	Falcini et al., 2012	10 ⁴	< 1 Year	Rivers	Product	TSS	Used remote estimates of TSS to examine sedimentation in wetlands and link them to hydrodynamics with implications for wetland restoration

1415

1416

Table S2. Summary of studies using remote sensing to analyze impacts and drivers of water quality and classified as water quality science papers within the analysis.